

Review

# A Review on Design Parameters for the Full-Cell Lithium-Ion Batteries

Faizan Ghani , Kunsik An  and Dongjin Lee  \*<sup>1</sup> School of Mechanical and Aerospace Engineering, Konkuk University, 120 Neungdong-ro, Gwangjin-gu, Seoul 05029, Republic of Korea<sup>2</sup> Department of Mechanical Engineering, Sejong University, 209 Neungdong-ro, Gwangjin-gu, Seoul 05006, Republic of Korea

\* Correspondence: djlee@konkuk.ac.kr; Tel.: +82-2-450-0452

**Abstract:** The lithium-ion battery (LIB) is a promising energy storage system that has dominated the energy market due to its low cost, high specific capacity, and energy density, while still meeting the energy consumption requirements of current appliances. The simple design of LIBs in various formats—such as coin cells, pouch cells, cylindrical cells, etc.—along with the latest scientific findings, trends, data collection, and effective research methods, has been summarized previously. These papers addressed individual design parameters as well as provided a general overview of LIBs. They also included characterization techniques, selection of new electrodes and electrolytes, their properties, analysis of electrochemical reaction mechanisms, and reviews of recent research findings. Additionally, some articles on computer simulations and mathematical modeling have examined the design of full-cell LIBs for power grid and electric vehicle applications. To fully understand LIB operation, a simple and concise report on design parameters and modification strategies is essential. This literature aims to summarize the design parameters that are often overlooked in academic research for the development of full-cell LIBs.

**Keywords:** Li-Ion batteries; design parameters; electrodes; electrolytes; electrochemical reaction mechanism; physicochemical properties



**Citation:** Ghani, F.; An, K.; Lee, D. A. Review on Design Parameters for the Full-Cell Lithium-Ion Batteries. *Batteries* **2024**, *10*, 340. <https://doi.org/10.3390/batteries10100340>

Academic Editor: Shaozhan Huang

Received: 1 August 2024

Revised: 19 September 2024

Accepted: 23 September 2024

Published: 25 September 2024



**Copyright:** © 2024 by the authors. Licensee MDPI, Basel, Switzerland. This article is an open access article distributed under the terms and conditions of the Creative Commons Attribution (CC BY) license (<https://creativecommons.org/licenses/by/4.0/>).

## 1. Introduction

Environmental pollution has been minimized through campaigns aimed at reducing harmful and residual waste materials from energy storage techniques. According to 2020 reports from the China Energy Storage Alliance (CNESA) database, hydropower energy sources, primarily pumped hydro storage systems, account for 92.6% (171.03 GW) of the total energy storage capacity. In contrast, electrochemical energy storage systems, which produce electrical energy from chemical reactions, account for the remaining 5.2% (9.6 GW) of all energy technologies. Along with fuel cells and supercapacitors, batteries are the main electrochemical energy storage system, collectively accounting for 89% (8.5 GW) of the electrochemical energy capacity [1,2]. They store energy in the form of ions and electrons produced during the charge process and are the primary energy storage method for consumer products such as portable electronic gadgets, smartphones, tablets, laptops, and even electric vehicles. The first lithium-ion battery (LIB), invented by Exxon Corporation in the USA, was composed of a lithium metal anode, a  $TiS_2$  cathode, and a liquid electrolyte composed of lithium salt ( $LiClO_4$ ) and organic solvents of dimethoxyethane (glyme) and tetrahydrofuran (THF), exhibiting a discharge voltage of less than 2.5 V [3,4]. LIBs were designed to include a high-potential cathode material, a low-potential anode material, and an electrolyte with a sufficiently wide potential window to facilitate ion transport. Sony Corporation's LIBs exploited a graphite anode (specific capacity of 372 mAh/g), a  $LiCoO_2$  cathode (specific capacity of 140 mAh/g), and an electrolyte containing  $LiPF_6$  salt in an EC:DEC/DMC solvent, resulting in a working voltage of approximately 3.0 V [5,6].

Increasing energy consumption demands LIBs to have a high voltage window and efficient electrode materials to provide high energy density. Consequently, significant research efforts have been focused on improving energy density, power density, calendar life, thermal stability, and reducing maintenance costs for LIBs.

Numerous studies have been conducted to investigate the development and performance enhancement of LIBs thereby. Such enhancement includes the aging mechanisms, thermal stability responses, and heat generation during the charge/discharge processes of LIBs [7–9]. Most studies have summarized the performance enhancement of LIBs based on one to three experimental design parameters. For that, a design of experiment was suggested to perform the experiment effectively [10]. Many electrode materials have been specifically designed to maximize specific capacities and performance to meet practical consumer demands. These materials are categorized based on their nature, crystallography, and electrochemical reaction mechanisms. Investigations into their crystallography, mechanical, physicochemical, and electronic properties, as well as their impact on electrochemical performance, have been summarized in various reports [11–13]. Furthermore, different synthesis techniques, mechanisms, and modification routes have been explored to enhance the electrochemical responses of various electrode materials [14–16]. These studies highlighted the importance of understanding LIBs at the full cell level and emphasized the need for comprehensive exploration of the thermodynamics and reaction kinetics of LIBs [17,18]. The individual aspects correspond to electrochemical reaction mechanisms, design of electrode materials, various synthesis routes, their effect on morphology and particle size reduction, surface modification techniques, thermal response, and other parameters for the progress of LIBs [14,19–21]. Although most studies are experimental approaches, computational approaches have also been explored to develop mathematical models of thermodynamics and electrochemical reaction kinetics of LIBs, aiming at optimization of various parameters [17,22]. The computational optimization of full-cell design parameters has been aimed at maximizing specific energy density [23]. Lain et al. investigated the commercial lithium-ion cells of various production companies and reported the practical design strategies for high-power LIBs [24]. Similarly, many reports on the types of electrolytes and their modifications to enhance the charge transference and electrochemical potential window have been discussed and summarized [25,26].

Recently, design methodology was suggested in terms of energy density and cost of LIBs for electric vehicles using the computer simulation models [27]. Furthermore, recent material development progresses were reviewed for high-voltage LIBs [28]. Specifically, the design of the electrode material was comprehensively reviewed, but discussion was limited to organic materials [29]. While the existing literature covers these individual components of LIBs, there is a need for a comprehensive review that delves into experimental findings and explains key design parameters and factors affecting the efficiency and energy density of full-cell LIBs. This review aims to scrutinize the crucial design parameters necessary for achieving high energy density full-cell LIBs. Additionally, it summarizes the latest research results and strategies for designing various parameters and provides a detailed discussion on the critical factors influencing the performance of full-cell LIBs.

## 2. Working Principle of LIBs

The LIB generally consists of a positive electrode (cathode, e.g., LiCoO<sub>2</sub>), a negative electrode (anode, e.g., graphite), an electrolyte (a mixture of lithium salts and various liquids depending on the type of LIBs), a separator, and two current collectors (Al and Cu) as shown in Figure 1. In LIBs, energy is stored and released through the movement of Li<sup>+</sup> ions between the anode and cathode. When LIB is charged, as depicted in Figure 1a, lithium ions migrate through the electrolyte from the cathode to the anode, where they are stored. LIBs are typically in a charged state with Li<sup>+</sup> ions stored within the crystal structure of the anode. During discharge, as demonstrated in Figure 1b, Li<sup>+</sup> ions are released from the anode, and the battery provides energy to an external load. Positively charged lithium ions move through the electrolyte from the anode to the cathode via the separator. It

generates free electrons at the anode, leading to electric current at the load. Possessing porous structure, the separator blocks electron flow but allows ion movement within the electrolyte. The efficiency and lifespan of the battery depend on the quality of materials used and the management of ion transfer. The voltage of the battery is determined by the chemical potential difference between the cathode ( $\mu_c$ ) and the anode ( $\mu_a$ ), which is influenced by the electrochemical potential window of the electrolyte. The energy density of a battery, indicating how much energy it can store, is generally expressed in watt-hours per kilogram (Wh/kg). Power density, reflecting the rate at which energy is delivered, is expressed in watts per kilogram (W/kg). Energy density pertains to the total energy stored (specific capacity), while power density refers to the effective use of that energy to perform work [19,30].

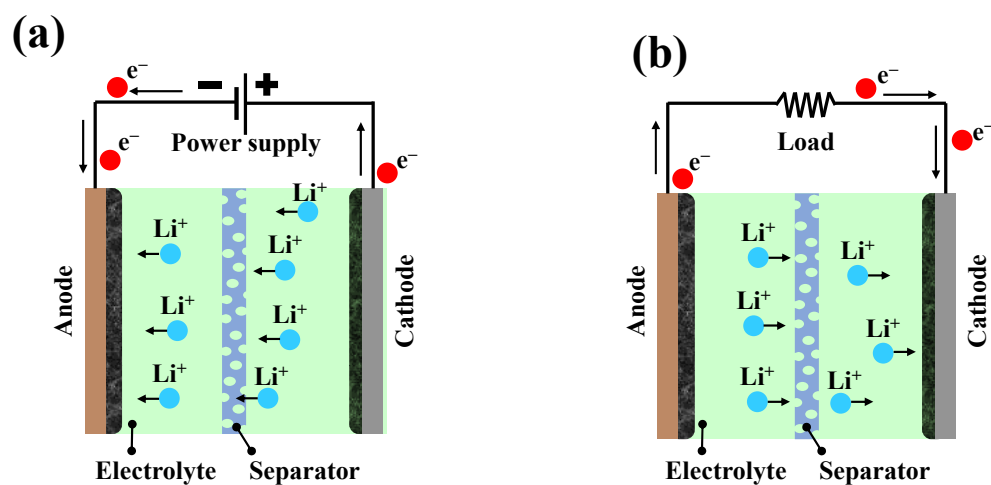


**Figure 1.** Working principle of the full-cell LIBs in case of (a) charging and (b) discharging.

### 3. Design Parameters for Full-Cell LIBs

The LIBs must meet the requirements of LIBs, such as voltage, current, and capacity, depending on the application. They also fit well in the space where the battery should be installed inside the final products, such as a laptop, smartphone, tablet, etc. The installed LIBs should be operated safely under use environments. To remain competitive in the market, finally, the LIBs should be fabricated and supplied at low cost. To meet such requirements, designing full-cell LIBs requires a comprehensive understanding of various design parameters suggested in this review. They include parameters such as form factor, material choices and types, the performance of main components, and productivity/cost as depicted in Figure 2. The form factor, such as geometry and dimension of the battery, ensures geometrical compatibility with electronic products. The choice and type of materials are most crucial for the design of full-cell LIBs, as they influence factors such as energy storage capacity, electrochemical reaction mechanisms, compatibility among components, performance of main components, and cost. Furthermore, the performance of the components of LIBs involves various factors that require thorough evaluation using advanced technological tools to understand their interdependencies. This performance depends on the compatibility of cell components and their effective interaction, the electrochemical potential window, mass loading (N/P ratio), reaction chemistry, intrinsic conductivity, and productivity. Finally, productivity directly influences the cost of full-cell LIBs, assuring market competitiveness. It is noted that these design parameters are closely related to each other, so that thorough consideration should be given when designing the LIBs.

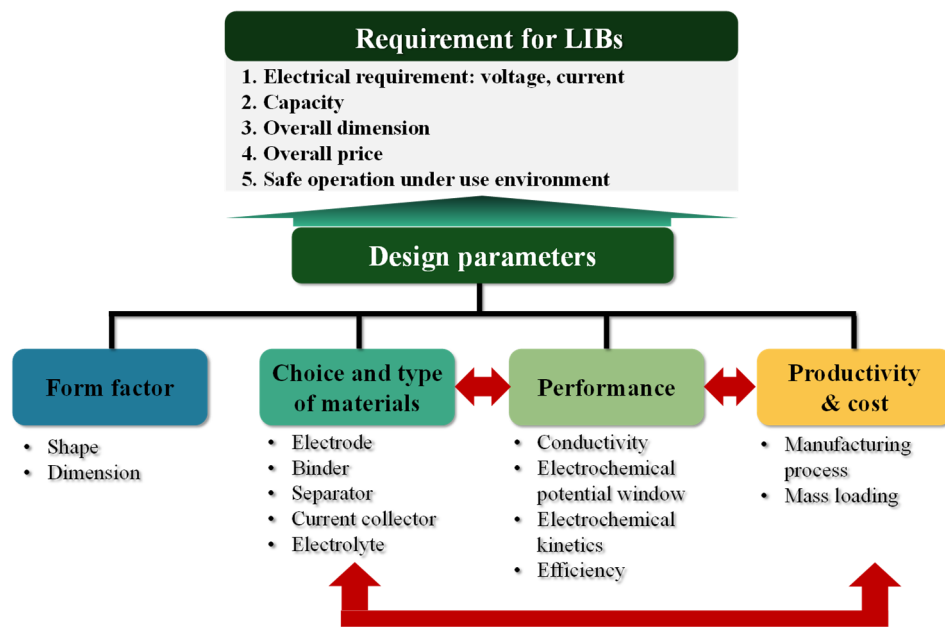


**Figure 2.** Design parameters for the full-cell LIBs discussed in this work.

### 3.1. Form Factor

The form factors of full-cell LIBs are essential design parameters, referring to attributes such as size, shape, volume, and weight. Size refers to the actual physical dimensions, including height, width, and thickness, while shape refers to the geometry of the battery, which can be coin-type, cylindrical, prismatic, or pouch-shaped, as shown in Figure 3. Volume indicates the space the battery occupies, and weight is the combined weight of various cell components, influenced by mass loading and the total number of cells. In full-cell battery design, therefore, the form factor is very elementary since it affects how the battery fits into devices, affects energy density, and influences overall performance. Particularly, the form factor is very important in applications like electric vehicles, mobile devices, and large-scale energy storage systems. The main cell types available on the market are summarized in Table 1. Limiting to coin-type cell configuration, CR2032, CR2016, or CR2025 can be chosen for single full-cell LIBs depending on the application. The full-cell configuration consists of the assembly of a casing (bottom and cap), a spacer, a wave-shaped O-ring, and a gasket to ensure a secure seal and prevent leakage during the charge/discharge process. Typically, these components are made of stainless steel, except for the gasket, which is made of polypropylene. The coin cell must be tightly sealed to prevent electrolyte leakage and gas emissions during operation.

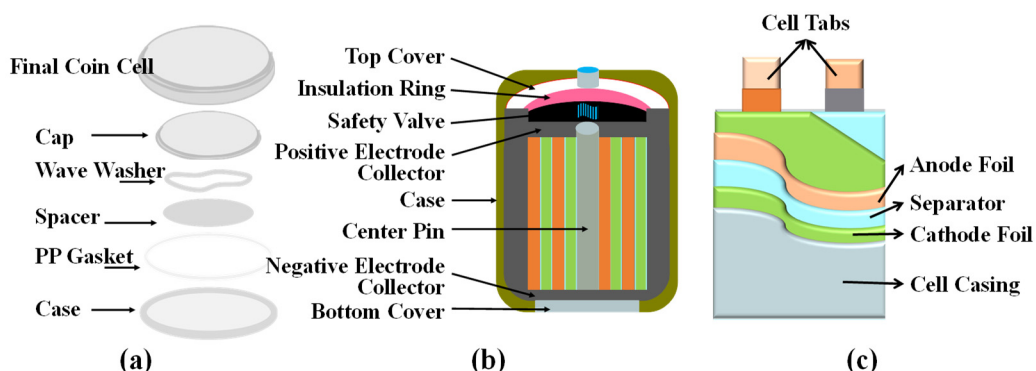


**Figure 3.** Various form factors of full-cell LIBs: (a) coin shape, (b) cylindrical shape, and (c) pouch-type.

**Table 1.** General properties of various form factors of LIBs.

Types of LIBs	Properties
Coin/Button Cell	<ul style="list-style-type: none"> <li>• Light weight, highly reliable, and cost effective</li> <li>• Wide operational window and long shelf life</li> <li>• High energy density and high cell voltage of ~3.0 V</li> <li>• Can be stacked for higher voltages with a high safety</li> <li>• Non-rechargeable (disposable/primary battery)</li> <li>• Delivers a low rate-capability and needs the assistance of a special holder</li> <li>• Operable between temperature range of <math>-30^{\circ}\text{C}</math> and <math>+60^{\circ}\text{C}</math></li> <li>• Applied in conventional calculators, camera, electronic watches, translators, etc.</li> </ul>
Cylindrical Cell	<ul style="list-style-type: none"> <li>• First mass produced LIBs with a high mechanical strength</li> <li>• Suitable for automated manufacturing at a lower cost</li> <li>• Small and round enclosed cylinder can that prevents swelling and prevents undesired reactions from the accumulation of gases</li> <li>• Poor heat management (thermodynamically unstable)</li> <li>• The internal pressure from side reactions evenly distributed along the cell circumference to extend their shelf-life, safety, and stability</li> <li>• Applied in laptops, electric vehicles, e-bikes, medical devices, and satellites, and is crucial for space exploration</li> </ul>
Pouch-Type Cell	<ul style="list-style-type: none"> <li>• Highly compact with small size cells (vulnerable to cause fires/explosions)</li> <li>• High efficiency and delivers highest power density</li> <li>• Relatively good safety performance and good ductility</li> <li>• High energy density and inexpensive to produce (cheaper cell than coin shaped and cylindrical cells)</li> <li>• Stable, safe to use, and with an enhanced cell weight</li> <li>• Comparatively degraded specific energy density</li> <li>• Gas-generated swelling</li> <li>• Standardized and knowledgeable automated production methodology increases the production rate</li> <li>• Applicable for high-end technology industry, portable applications such as mobile device, drones, and portable energy stations</li> </ul>

### 3.2. Choice and Types of Materials for Main Components

Materials themselves are the most fundamental design factors that determine the electrochemical potential window, reaction chemistry (including reaction kinetics and mechanisms), and the types of batteries (e.g., aqueous, non-aqueous, polymeric, or solid-state). They also influence the cyclability, thermal stability, and overall performance of full-cell LIBs. Thus, most research was conducted to develop novel structures of materials for the main components of full-cell LIBs shown in Figure 4. Since the inception of LIBs, full-cell components have been thoroughly studied, and research continues to identify improvements with emphasis on the materials. It is well known that the materials are key factors in facilitating electrochemical reactions that generate high specific capacity and energy density within the electrochemical potential window. In detail, the main components of LIBs include electrodes (anode and cathode), binders (polymeric material), current collectors (metal foil of Cu or Al), separators (polyolefin thin sheet), and electrolytes (a mixture of salts and liquids). The properties of these components—including their electronic and crystal structures, chemical, electrical, and mechanical characteristics and intrinsic conductivities—play a crucial role in developing favorable reaction chemistries, enhancing thermal and mechanical stability, and improving the performance of full-cell LIBs.

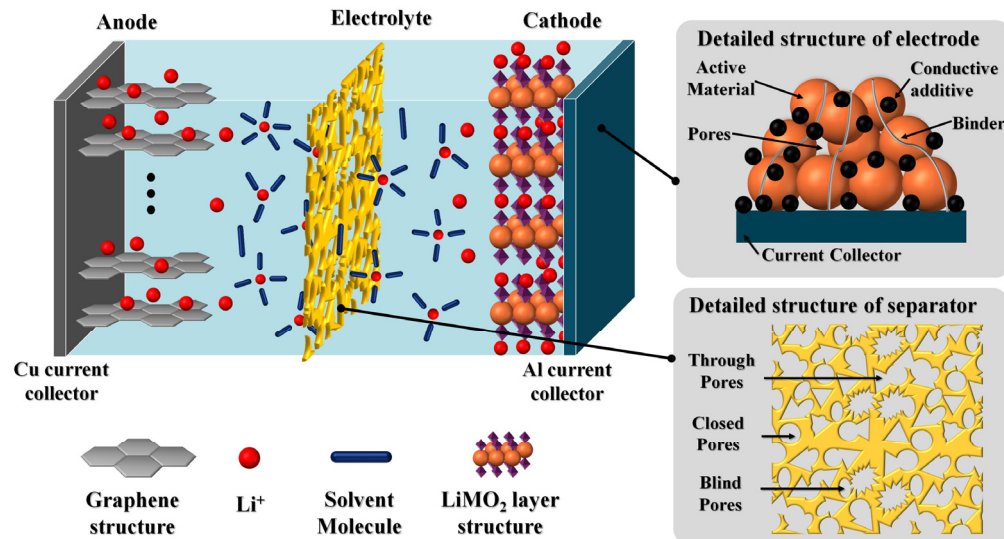


**Figure 4.** Detailed structure of main components of LIBs: each component has complex structures of several materials to enhance the performance.

### 3.2.1. Electrode

The electrode is one of the primary components of LIBs, determining the electrochemical potential window, specific capacity, energy and power density, overall performance, and electrochemical reaction mechanism. As a result, the design and modification of electrode materials is crucial for achieving high energy and power densities. Ideally, the electrode should exhibit high intrinsic conductivity, a wide potential window, excellent cycle and rate performance, low cost, and robust stability and safety to improve the overall performance of LIBs. Over the years, two major design strategies, intrinsic and extrinsic, have been explored to achieve these desired properties for LIBs in terms of many aspects as shown in Figure 5.

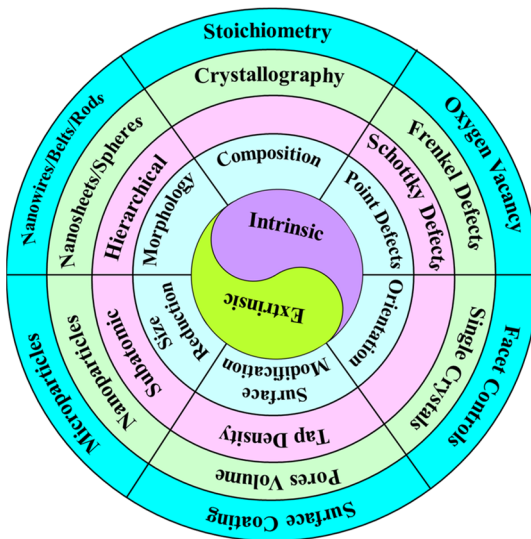


**Figure 5.** Two design strategies for electrode of LIBs: intrinsic vs. extrinsic.

The intrinsic design strategy primarily focuses on developing stoichiometric compositions, optimizing crystal defects, and controlling crystal orientation, which are discussed in detail.

- **Chemical compositions:** The chemical composition defines the crystal structure and governs key properties such as mechanical strength (adhesion/cohesion), stability

(structural, chemical, and thermal), phase transformation, and intrinsic conductivity (electrical and ionic). It also specifies the amount of  $\text{Li}^+$  ions that can be inserted or extracted from the crystal structure, directly impacting on the electrochemical properties of electrode materials [31–34]. Additionally, structural units, which represent the material's 'genes', provide insights into local chemical coordination and molecular chemistry, establishing the physical and chemical properties of the electrodes. Understanding the correlation between structural units and these physical/chemical properties offers critical evidence about charge-transfer characteristics, which are essential for intrinsic properties like structural/thermal stability, electronic/ionic conductivities, and  $\text{Li}^+$  ion transport. These properties are crucial for enhancing the electrochemical performance of LIBs [35]. Therefore, it is essential to design and develop structurally tunable electrode materials that can accommodate additional  $\text{Li}^+$  ions, improve intrinsic conductivities, expand the voltage window, enhance diffusion kinetics, and provide excellent electrochemical performance for LIBs.

- **Point defects:** Similarly, point defects such as Frenkel defects (where an atom migrates from its lattice site to an interstitial site, creating an interstitial defect), Schottky defects (which involve the simultaneous presence of cation and anion vacancies), and oxygen vacancies (absence of oxygen atoms or presence of hydroxyl ions within the crystal structure) play a significant role in defining the local structure of electrode materials. These defects can enhance intrinsic conductivity, improve thermal and structural stability, facilitate pseudo-capacitive kinetics, limit volume expansion, and boost the electrochemical performance of LIBs. Generally, electrode materials with symmetric compositions tend to act as semiconductors, while non-stoichiometric materials (doped or defect-induced) behave like metals, which helps alleviate structural, chemical, and thermal changes [36–39]. However, the effect of oxygen vacancies, compared to Frenkel and Schottky defects, has been insufficiently studied and further investigations are required for the development of innovative LIBs.
- **Crystal Orientation:** Crystal orientation influences specific facets, crystal structures, and surface energies, which in turn affect thermodynamics and reaction kinetics at the surface/interfaces. In batteries, supercapacitors, and fuel cells, physical and chemical interactions at the interfaces play an important role in promoting electrochemical energy storage activities [40]. Additionally, single crystals, which offer advantages such as a small specific surface area, excellent structural stability, high mechanical and thermal stability, superior reaction homogeneity, and good crystallinity, have been studied for their impact on crystal orientation. These studies aim to significantly enhance the electrochemical performance of electrode materials for LIBs, including safety, capacity retention, and cycle life. Electrode materials with low activation energy and substantial adsorption kinetics of crystal facets are promising for achieving high energy density and rate performance in LIBs [41–44]. The interest in exploring single crystal electrodes and their potential applications continues to grow, highlighting the need for advanced research methodologies to address future energy challenges.

On the other hand, the extrinsic design strategy fundamentally focuses on the effect of size reduction, morphological changes, and surface modifications of electrode materials.

- **Size reduction:** The particle size, size distribution, and shape of particles influence the contact area, diffusion resistance, diffusion path, energy density, and overall electrochemical performance of LIBs. Reducing particle size shortens the transportation length of  $\text{Li}^+$  ions, decreases the  $\text{Li}^+$  ion diffusion barrier, enhances ionic diffusion, increases the contact area among electrode active materials, current collectors, and electrolytes, and ensures the electroactivity of the electrode materials. However, smaller particle sizes also increase the surface area, which can promote electrochemical activity and lead to more side reactions, potentially causing thermal issues and internal short circuits in LIBs [21,45,46]. Particle size distribution affects the physical and chemical properties and overall surface energy activity of electrode materials. A broad size distribution results in high energy density but poor cell homogeneity due to particle

size variance and surface energy differences. In contrast, a uniform size distribution, although challenging to produce, offers stable electroactivity by reducing stress strains during the charging process, thereby improving the cycle performance of LIBs [47,48]. Additionally, particle shape directly affects the effective surface area and mass flow properties, particularly the tap density, which influences the  $\text{Li}^+$  ion diffusion channels and reaction kinetics, enhancing the cycle performance of LIBs. However, particles derived from single-crystal structures are expensive and difficult to manufacture and handle, requiring a highly regulated reaction environment [49–51].

- **Morphological change:** The shape and morphology of electrode materials affect various factors such as porosity, tap density, diffusion pathways, surface area, and interfacial contact area. These factors comprehensively lower the activation energy for electrochemical reactions, shorten the transportation length for  $\text{Li}^+$  ions, enhance diffusivity and electroactivity, and improve specific capacity and rate capability, ultimately determining the electrochemical performance for energy storage applications [52,53]. Several morphologies, including nanosheets, nanowires/rods/belts/tubes, hierarchical nanostructures, microcubes, microspheres, and micro-flowers, have been developed depending on synthesis and calcination conditions. Nanowires/rods/belts/tubes and nanosheets, with improved compact density, provide unidirectional diffusion pathways for  $\text{Li}^+$  ions. In contrast, microspheres/flowers, urchin-like structures, and 3D microspheres/microcubes with sizes around 5–10  $\mu\text{m}$  increase electrode packing density, accommodate inactive components (binders and conductive additives used in slurry fabrication), offer extensive surface-active sites for electrolyte penetration, and promote  $\text{Li}^+$  ion diffusion, resulting in high energy density for LIBs [54–56]. However, micron-sized particles can limit the rate performance and power density of LIBs by extending the diffusion pathways for  $\text{Li}^+$  ions. Additionally, large cracks and deformations often appear between grain boundaries and at the electrode surface due to the accumulation of significant stresses during the charging process. These issues restrict electronic and ionic conductivity, leading to capacity fading, electrode detachment, and cell degradation [57,58].
- **Surface modification:** Surface modification is an accessible, cost-effective, and widely applied strategy and it is achieved through techniques such as surface coating, etching, and ion doping. These methods enhance ionic conductivity and create surface-active sites that facilitate electrolyte penetration, which is crucial for forming a solid electrolyte interface (SEI) layer. This layer helps buffer volume expansion and contraction, maintaining structural integrity and mitigating capacity fading during cycling [14,59,60]. Consequently, it is highly desirable to prepare electrodes with high voltage, high energy density, low cost, excellent intrinsic conductivity, and robust structural, chemical, and thermal stability. Additionally, electrodes should feature various morphologies with high surface area and porous characteristics. Surface modification techniques, including coating with carbonaceous materials or metal oxides, surface treatment (such as acid/base or metal oxide etching), and ion doping, are essential for enhancing electronic and ionic conductivity and developing coating layers. These modifications help alleviate volume changes, suppress microstrains in the crystal structure, and improve surface adsorption characteristics for additional  $\text{Li}^+$  ions, thus promoting the electrochemical performance of LIBs. Electrodes, whether designed intrinsically or extrinsically, are classified into various types based on the electrochemical reaction chemistry during the cycling process. Numerous reports detail the cathode and anode materials, synthesis methodologies, modifications, and investigations into electrochemical reaction mechanisms [24,61–63].

Tables 2 and 3 summarize the anode and cathode materials used in previous studies, respectively. Even though researchers do not use either of the two strategies, the above-mentioned electrode design factors were investigated to design better anode and cathode electrodes.

**Table 2.** Classifications, advantages, and disadvantages of various cathode materials for LIBs.

Class	Types	Advantages	Disadvantages	Refs
Co-based oxides		<ul style="list-style-type: none"> <li>• High capacity</li> <li>• High energy density</li> <li>• Good cycle life</li> <li>• Good rate performance</li> <li>• High power density</li> </ul>	<ul style="list-style-type: none"> <li>• Highly toxic</li> <li>• High cost</li> <li>• Chemical/thermal instability</li> <li>• O<sub>2</sub> evolution</li> </ul>	[64–66]
	Ni-rich oxides	<ul style="list-style-type: none"> <li>• High capacity</li> <li>• Safety</li> <li>• Middle cost</li> <li>• Good cycle life</li> <li>• Chemical/structural stability</li> <li>• Good conductivity</li> <li>• Low toxicity</li> </ul>	<ul style="list-style-type: none"> <li>• Poor performance</li> <li>• Volume expansion</li> <li>• Structural/thermal instability</li> <li>• O<sub>2</sub> evolution</li> <li>• Li deficiency</li> <li>• Phase transition</li> <li>• Ni+4 existence</li> </ul>	
Layered Oxides	Li-rich oxides	<ul style="list-style-type: none"> <li>• High capacity</li> <li>• High energy density</li> <li>• Safety</li> <li>• Anions activity</li> <li>• Extra Li insertion</li> </ul>	<ul style="list-style-type: none"> <li>• Poor cycle and rate performance</li> <li>• High irreversible capacity</li> <li>• Voltage hysteresis</li> <li>• O<sub>2</sub> evolution</li> <li>• Phase transition</li> </ul>	[71–74]
		<ul style="list-style-type: none"> <li>• Low cost</li> <li>• High capacity</li> <li>• Good rate performance</li> <li>• Structural stability</li> <li>• Thermal Stability</li> <li>• High voltage</li> </ul>	<ul style="list-style-type: none"> <li>• Poor cycle life</li> <li>• Poor conductivity</li> <li>• Irreversible phase formation</li> <li>• Poor reaction kinetics</li> <li>• Mass production</li> </ul>	
Spinal Oxides	LiM <sub>2</sub> O <sub>4</sub> (M=Co, Mn, Ni)	<ul style="list-style-type: none"> <li>• Low cost</li> <li>• High voltage</li> <li>• Good rate performance</li> <li>• Abundant Mn</li> <li>• Non-toxic/safety</li> <li>• Fast diffusion kinetics</li> <li>• Structural/Thermal stability</li> </ul>	<ul style="list-style-type: none"> <li>• Poor cycle life and energy density</li> <li>• Voltage hysteresis</li> <li>• Mn dissolution</li> <li>• Anions reduction</li> <li>• Jahn–Teller distortion</li> <li>• Restrict high energy density applications</li> </ul>	[75–77]
	Phosphate oxides	<ul style="list-style-type: none"> <li>• Low cost</li> <li>• Excellent cycle life</li> <li>• Good rate performance</li> <li>• High capacity</li> <li>• High safety</li> <li>• Structural/thermal stability</li> <li>• High voltage</li> <li>• Prevent O<sub>2</sub> evolution</li> </ul>	<ul style="list-style-type: none"> <li>• Poor conductivity</li> <li>• Low volumetric energy density</li> <li>• High processing cost</li> <li>• Low practical capacity</li> <li>• Capacity fading</li> <li>• Anti-site defects</li> <li>• Poor reaction kinetics</li> </ul>	
Polyanionic	Silicate oxide	<ul style="list-style-type: none"> <li>• Low cost</li> <li>• High safety</li> <li>• High specific capacity</li> <li>• Availability</li> <li>• 2D Li-ion diffusion channel</li> </ul>	<ul style="list-style-type: none"> <li>• Poor conductivity</li> <li>• Poor rate performance</li> <li>• Structural instability</li> <li>• Severe capacity fading</li> </ul>	[81–84]
	Borate oxides	<ul style="list-style-type: none"> <li>• High theoretical specific capacity</li> <li>• Safety</li> <li>• High voltage</li> </ul>	<ul style="list-style-type: none"> <li>• Structural instability</li> <li>• Poor ionic conductivity</li> <li>• Poor cycle life</li> </ul>	
Tavorites		<ul style="list-style-type: none"> <li>• Good rate performance</li> <li>• Structural/Thermal stability</li> <li>• Strong O-P bond</li> </ul>	<ul style="list-style-type: none"> <li>• Low capacity retention</li> <li>• Low Li recovery</li> <li>• Low columbic efficiency</li> </ul>	[85,86]

**Table 3.** Classifications, advantages, and disadvantages of various anode materials for LIBs.

Class	Types	Advantage	Disadvantage	Refs
	Carbonaceous	<ul style="list-style-type: none"> <li>• Low cost, Abundance</li> <li>• High safety</li> <li>• Good cycle life</li> <li>• Good rate performance</li> <li>• Good working potential</li> <li>• Structural stability</li> <li>• High electronic conductivity</li> </ul>	<ul style="list-style-type: none"> <li>• Low capacity</li> <li>• High irreversible capacity</li> <li>• Low columbic efficiency</li> <li>• Dendrite formation</li> <li>• Internal short circuit</li> </ul>	[19,61,91–94]
Insertion/ Extraction	Ti oxides	<ul style="list-style-type: none"> <li>• Low cost</li> <li>• High safety/non-toxic</li> <li>• Abundant sources</li> <li>• High cycle performance</li> <li>• High rate performance</li> <li>• Chemical/structural stability</li> </ul>	<ul style="list-style-type: none"> <li>• Poor electronic conductivity</li> <li>• Poor ionic conductivity</li> <li>• Low energy density</li> <li>• Low capacity</li> </ul>	[19,61,92–94]
Alloy/de-Alloy	Si, Ge, Sn, Sb, SnO, SiO, Zn, etc.	<ul style="list-style-type: none"> <li>• Abundance/low Cost</li> <li>• Good safety/non-toxic</li> <li>• Excellent capacity</li> <li>• High energy density</li> <li>• Good rate capability</li> <li>• Good electrical conductivity</li> <li>• Good working potential</li> <li>• Large volumetric capacity</li> </ul>	<ul style="list-style-type: none"> <li>• Poor cyclability</li> <li>• Sluggish reaction kinetics</li> <li>• Large volume expansion</li> <li>• Pulverization</li> <li>• Large capacity fading</li> <li>• High irreversible capacity</li> <li>• Structural instability</li> <li>• Unstable SEI</li> <li>• Highly toxic</li> </ul>	[19,61,92–94]
	Metal oxides	<ul style="list-style-type: none"> <li>• Low cost/ Availability</li> <li>• Eco-friendly/Good cycle</li> <li>• High capacity</li> <li>• High energy density</li> <li>• Rate performance</li> </ul>	<ul style="list-style-type: none"> <li>• Poor conductivity</li> <li>• Large potential hysteresis</li> <li>• Low C.E and unstable</li> <li>• SEI formation</li> <li>• High irreversible capacity</li> <li>• Large capacity fading</li> <li>• Volume expansion</li> </ul>	[12,16,61,92–96]
Conversion	Chalcogenides	<ul style="list-style-type: none"> <li>• Eco-friendly/low cost</li> <li>• Low working potential</li> <li>• Low polarization</li> <li>• High capacity</li> <li>• High energy density</li> </ul>	<ul style="list-style-type: none"> <li>• Poor conductivity</li> <li>• Sluggish reaction kinetics</li> <li>• Low potential hysteresis</li> </ul>	[19,61,92–96]

### 3.2.2. Binders

LIB electrodes are typically fabricated by coating a slurry composed of active material, conductive additives, and non-conductive binder onto a current collector foil. The role of the binder in LIBs is as follows: The binder primarily maintains the structural integrity of the electrode materials by binding the active material particles (such as lithium cobalt oxide or graphite) and conductive additives (such as graphite, hard carbon, Super P, KS6, etc.) together. Binders also ensure good electrical contact within the electrode by maintaining a connection between the active material particles and the current collector. Finally, binders accommodate the stress and volume changes that occur in electrode materials during charge and discharge cycles.

Exothermic reactions might degrade the binder material, leading to thermal instability and potential internal short circuits in LIBs. Typically, being electrical insulators, binders should not hamper the movement of  $\text{Li}^+$  ions to preserve the ionic conductivity, which is essential for charging efficiency and operation. The binder must absorb these changes without cracking or losing contact with the active material or current collector, which directly contributes to battery durability and cycle life. Therefore, it is essential to design

binder materials with high mechanical strength, good adhesion properties, accessibility, low cost, recyclability, non-toxicity, and electrochemical stability [97–99]. Moreover, the binders must be chemically stable and inert in the battery's electrolyte to avoid degradation, which can compromise the electrode structure and lead to battery failure. Inhomogeneous distribution of conductive phases can limit electronic and ionic conductivities and affect the mechanical contact of the electrodes. Binders help create a uniform slurry, ensuring smooth coating onto the current collector. This uniformity is vital for consistent battery quality and performance. Furthermore, binders contribute to the battery's environmental stability, protecting electrodes from humidity, temperature fluctuations, and other external factors.

Table 4 summarizes various binder materials in terms of advantages and limitations. Various types of binder materials—aqueous, non-aqueous, solvent-based polymeric, and gel framework types—have been developed to provide improved contact and electrochemical stability during charging and discharging processes. They also prevented aggregation of active material particles and capacity fading. The overall thermal stability of LIBs encompasses the thermal stability of electrodes, separators, electrolytes, and the thermodynamic stability of the binder [100,101]. Therefore, binder materials with high electronic conductivity, mechanical strength, ductility, surface compatibility, self-healing properties, and effective ion transport capabilities significantly enhance the electrochemical performance, thermal and structural stability, and cycling stability of LIBs.

**Table 4.** Types and general properties of various binder used for LIBs.

Types	Materials	General Properties	Refs
Aqueous	Na based CMC, SBR, Chitosan, Alginate, etc.	<ul style="list-style-type: none"> <li>Low-cost and pollution free</li> <li>Processability with no humid issues</li> <li>Evaporate solvent fast</li> <li>Average swelling tendency and Li<sup>+</sup> ion conductivity</li> <li>Strong chelation and adhesion properties</li> </ul>	[102–104]
Non-aqueous	PVDF, SBR, NBR, CMC, PAN, CA, etc.	<ul style="list-style-type: none"> <li>Expensive, toxic, and humid sensitivity issues</li> <li>Large swelling resulting peeling off the active mass from current collector during cycling process</li> <li>Fast capacity fading for anode materials</li> <li>Insufficient binding/chelation properties</li> </ul>	[105,106]
Polymer	CMC, SBR, PVA, PVD, PVDF, SA, FPI, AR/CMC, Lignin, Sericin protein, etc.	<ul style="list-style-type: none"> <li>Excellent distribution of electrode components</li> <li>Inhibited dissolution of transition metal ions</li> <li>Good Li<sup>+</sup> ion conductivities</li> <li>Uniform passivation of high-voltage cathodes</li> <li>Radical quenching ability</li> <li>High cohesive/adhesion and mechanical properties</li> <li>Scavenging HF and alleviating crystals of active materials</li> </ul>	[100,107,108]
Hybrid	PAA-PAI, GO-StC, β-CDp, Natural polymer, WS-PS, etc.	<ul style="list-style-type: none"> <li>Good adhesion and mechanical properties</li> <li>Strong chelation and binding properties</li> <li>Negligible swelling and no peeling off the active mass from current collector</li> <li>Cost effective, eco-friendly, abundant, and have low viscosity</li> <li>Processability and uniformity of coating</li> </ul>	[109,110]

### 3.2.3. Separators

The separator is also a crucial component of LIBs, as it isolates the electrodes, facilitates ionic diffusion pathways, prevents electronic conduction, and mitigates internal short circuits and thermal runaway. It plays a key role in defining the energy density, power density, and safety of LIBs. Separators must be chemically and thermally stable at elevated temperatures, electrically inactive, and resistant to degradation during battery operation [111]. Various types of separators have been explored and classified into categories such as (i) polyolefin films (e.g., PP, PE, PEI, PDA, PMMA, and glass fibers), (ii) thermally conductive materials (e.g., AlN/PP and BN/PP/C), (iii) carbon materials (e.g., cellulose-derived carbon, graphene, PDA/Gr-CMC, and Na-alginate), (iv) metals (e.g., Cu/PP, Si/PP, and Nb/PP), and (v) metal oxides (e.g.,  $\text{Al}_2\text{O}_3/\text{PP}$ ,  $\text{SiO}_2/\text{PP}$ , and  $\text{ZrO}_2/\text{PP}$ ) [112]. The separator should facilitate ion transport through its pores, improve interfacial compatibility, and enhance the safety of LIBs. An inert surface of separators can weaken the electrode-separator interface, leading to longer diffusion paths, irregular Li plating, dendrite formation, and thermal runaway. Therefore, optimizing ionic and physical contact while minimizing voids is essential to improving interfacial compatibility, preventing dendrite formation, and reducing thermal shrinkage in separators for advanced battery systems [113]. Key designing parameters of the separator include thickness, porosity, mean pore size, tortuosity, permeability, wettability, thermal stability, and mechanical properties.

- **Thickness:** The thickness of a separator typically ranges from 20 to 50  $\mu\text{m}$ , influencing the stability, mechanical properties, overall weight, and cell resistance of LIBs. For example, the commercially available Celgard 2400 separator has a thickness of 25  $\mu\text{m}$  [114].
- **Porosity:** Porosity is a crucial factor in determining mass transport, as it ensures sufficient  $\text{Li}^+$  ion conductivity and helps inhibit the formation of dendritic lithium. Common separators in the battery market typically exhibit around 40% porosity, which is defined as the ratio of the volume of pores to the apparent total volume of the pores. Porosity is typically measured by calculating the weight difference of the separator before and after soaking it in liquid, as shown below [115,116].

$$\text{Porosity}(\%) = \frac{(1 - \rho_m)}{\rho_p} \times 100 \quad (1)$$

$$\text{Porosity}(\%) = \frac{(W - W_o)}{\rho_L V_o} \times 100 \quad (2)$$

where  $\rho_m$ ,  $\rho_p$ ,  $W$ ,  $W_o$ ,  $\rho_L$ , and  $V_o$  represent the apparent density, separator material density, weight of void separator, weight of separator soaked in liquid, density of liquid, and geometric volume of separators, respectively.

- **Mean pore size:** The mean pore size is closely related to the size of  $\text{Li}^+$  ions, active ionic species in the electrolyte, and active mass components. Pore size controls the flow of  $\text{Li}^+$  ions, blocks lithium dendrites, and prevents short circuits. There exists a mean pore size of less than 1  $\mu\text{m}$  for a commercially viable and safe separator to allow  $\text{Li}^+$  ion transportation and block other active species. They can be classified into closed, blind, and through pores, as shown in Figure 4. Closed pores are fully enclosed without void spaces, while blind pores open to a void space on one side but are blocked on the other, trapping  $\text{Li}^+$  ions and potentially leading to dendrite formation. Pores with open void spaces and high permeability allow effective  $\text{Li}^+$  ion transport.
- **Geometric effect:** The geometric effect of pore morphology on the conductivity of  $\text{Li}^+$  ions under certain pressure differences is known as tortuosity. It describes the morphological changes in the pores of the separator. Pores exhibit various morphologies, including interconnected, network-type hierarchical structures, circular shapes, and

other microstructures. Tortuosity is the ratio of the mean path length that ions must travel through the pores to the direct straight-line distance as follows:

$$\text{Tortuosity}(\tau) = \text{Sqrt}\left(\epsilon \times \frac{R_s}{R_o}\right) \quad (3)$$

where  $\epsilon$  is porosity, and  $R_s$  and  $R_o$  are resistivity of separators before and after soaking in liquid, respectively. Permeability is calculated using Darcy's law, which describes the rate of fluid flow through a porous surface as follows:

$$\text{Average Velocity}(\mu) = \frac{-\kappa}{\eta \nabla P} \quad (4)$$

where  $\mu$  is average velocity,  $\eta$  and  $\nabla P$  are viscosity and applied pressure gradient of the fluid, respectively, and  $\kappa$  is permeability of separators.

- **Wettability:** It is a key aspect of the separator that directly influences the capacity and cycle retention of LIBs. A separator must quickly absorb electrolytes and initiate uniform  $\text{Li}^+$  ion transportation to prevent uneven  $\text{Li}^+$  ion deposition on the electrodes. The wettability of the separator is measured through contact angle analysis and assesses its affinity for liquid electrolytes by determining the angle formed between the separator surface and the electrolyte droplet.
- **Thermal stability:** Thermal stability is a crucial factor for ensuring the safety of LIBs. The separator must remain thermodynamically stable and withstand rising heat flux during battery operation under extreme conditions. When the separator shrinks or wrinkles at high temperatures, it leads to poor interfacial contact with electrodes, resulting in significant energy loss. Excessive heat flow can trigger thermal runaway and internal short circuits in the LIBs. To prevent these issues, the thermal shrinkage of the separator must be kept below 5% after 60 min at 90 °C under vacuum and can be measured using the following equation:

$$\text{Thermal Shrinkage}(\%) = \left( \frac{A_i - A_f}{A_i} \right) \times 100 \quad (5)$$

where  $A_i$  and  $A_f$  indicate area of separators before and after heat treatment at a certain temperature, respectively [114–116]. Furthermore, the separator must possess a shutdown effect, where the pores are blocked once abnormal heat flow is detected. This feature prevents direct contact between electrodes, inhibiting thermal runaway and internal short circuits. In addition, the separator should be non-flammable, ideally flame retardant, because if thermal runaway occurs, a flammable separator could catch fire, potentially leading to a battery explosion [113,117].

- **Mechanical properties:** The mechanical properties (e.g., mechanical strength, strain percentages, compression percentages) play a crucial role in determining the stability of separators and LIBs. During cell assembly, the interaction between electrolytes and separators causes mechanical softening and swelling under compression. Battery operation induces volume expansion in the electrode's active materials, exerting pressures of up to ~5 MPa. Under such stresses, the elastic modulus of the separator decreases, reducing its tolerance, altering its microstructure, hindering ionic conductivity, and leading to swelling. This compromises stability, promotes dendritic Li formation, and increases the risk of internal short circuits in LIBs [118,119].

Therefore, separators with thermal stability, high porosity, and strong mechanical properties must be designed, taking into account the aforementioned critical parameters to achieve high-energy and high-safety LIBs.

### 3.2.4. Current Collector

Current collectors, though non-active materials in full-cell LIBs, play a crucial role in providing mechanical support for electrodes, enhancing electrical conductivity, corrosion resistance, and reducing contact resistance. These, in turn, improve the specific capacity, efficiency, cycle stability, and rate performance of LIBs. Comprising the second-largest weight percentage (15%) of the total weight of a full-cell LIB, excluding the case, efforts to reduce their thickness have been made to increase energy density. The essential design parameters for current collectors include electrochemical stability, density, mechanical strength, electrical conductivity, sustainability, and cost [120,121]. Furthermore, the choice of material, availability, recyclability, and cost are other important factors when designing current collectors for full-cell LIBs [122]. Each of these design parameters is discussed in detail below.

- **Electrochemical stability:** It is essential to keep the stable reduction/oxidation environment during the battery operation as cathode and anode require high and low electrochemical potentials in LIBs, respectively. Any undesired reactions between the current collector and the electrolyte at these extremes can destabilize the system, leading to capacity fading and a shortened cycle life. Therefore, selecting a current collector with excellent electrochemical stability is crucial for achieving LIBs [123].
- **Density:** Current collectors with low densities are advantageous for reducing weight and cost, which can enhance the energy density of LIBs. Furthermore, high mechanical strength is crucial for preserving the integrity of the electrode materials and ensuring strong bonding with the current collector, electrodes, and polymer binder materials.
- **Mechanical strength:** A current collector with high mechanical strength helps suppress volume expansion, prevent electrode pulverization and delamination, and maintain the integrity of active components, thereby enhancing cycle stability and prolonging the cycle life of LIBs [94].
- **Electrical conductivity:** The electrical conductivity of the current collector and the interfaces between the electrode and current collector is crucial for LIB performance, as electrons generated at the electrodes travel through the current collector to the external circuits. A current collector with high electrical conductivity improves energy efficiency and minimizes heat generation, thus reducing the loss of chemical/electrical energy as heat during battery operation [124].

The choice of materials for current collectors significantly impacts the electrochemical performance, electrode stability, and high-rate performance of LIBs. Various materials, such as copper (Cu), aluminum (Al), titanium (Ti), nickel (Ni), stainless steel, and carbonaceous materials, are used as current collectors. These materials can be processed into different forms, including foils, foams, meshes, etched surfaces, and coated layers. Chemical treatments like etching and coating can notably improve surface roughness, corrosion resistance, and contact resistance, thereby enhancing the overall performance of LIBs [125,126].

### 3.2.5. Electrolyte

Electrolytes, as non-electroactive components, should not participate in redox reactions or allow electron flow. Their primary role in a battery system is to facilitate the ionic transportation of species generated during redox reactions at the electrodes and to serve as the medium for charge transfer. They also facilitate chemical reactions and accommodate thermal and mechanical variations to prevent damage or explosions of the battery system. Ionic transport in electrolytes has been extensively studied, with computational models suggesting that it occurs through mechanisms like migration, diffusion, and convection. These processes contribute to the flux density of dissolved species within the electrolyte [127]. Therefore, the electrolyte must exhibit the following characteristics to ensure proper electrochemical reactions in LIB full cells:

- **Ionic conductivity:** The electrolyte must enable efficient ion transport, meaning it should be highly conductive to ions. High ionic conductivity within the electrolyte

facilitates the rapid movement of ions between electrodes, promoting efficient charging and discharging of the LIB. This characteristic is crucial as it directly impacts the rate performance and power density of the LIB. Therefore, to achieve a high-rate and high-power density LIB, the electrolyte must exhibit excellent ionic conductivity.

- **Wide potential stability window:** The potential window of the electrolyte defines the range within which ions can effectively move between the cathode and anode. To ensure optimal performance, the electrolyte must support ionic movement from the highest occupied molecular orbital (HOMO) to the lowest unoccupied molecular orbital (LUMO) of the electrode materials. A broad potential window allows for a wider range of electrochemical reactions, enhancing the specific capacity, cycle life, and overall electrochemical performance of the LIB. Moreover, the potential window must remain stable during cycling to preserve the reaction chemistry, prevent thermal runaway, and maintain the structural and operational stability of the full-cell LIBs. Any fluctuation in this window can compromise the cell's performance and safety. Therefore, a stable and wide potential window is essential for achieving high-performance, long-lasting, and safe LIBs.
- **Chemically inert:** Electrolytes must be electrochemically inert and should not participate in the electrochemical reaction of the full-cell LIBs.
- **Low cost:** The electrolyte should be cost-effective and have easy accessibility.
- **Reducible:** The electrolyte must undergo reduction during the electrochemical reaction so that  $\text{Li}^+$  ions can transfer under the migration, diffusion, and convection phenomena.
- **Environment-friendly:** The electrolyte materials should be non-toxic and environment-friendly and should not cause any harm to human beings, animals, or the environment.
- **Electron insulator:** The electrolyte must block electron flow while allowing uninterrupted ionic transport. In other words, it should act as an electrical insulator, preventing electron involvement in any reactions during the electrochemical process.
- **High fluidity and low vapor pressure:**

The electrolytes are composed of metal salts and various solvents. Conducting salts must be fully dissolved to enhance ionic mobility and remain inert to the solvent and other battery components to prevent degradation. These salts should also be non-toxic, non-corrosive, and thermally stable to ensure safety during battery operation. Common salts used in LIBs include lithium perchlorate ( $\text{LiClO}_4$ ), lithium hexafluorophosphate ( $\text{LiPF}_6$ ), lithium bis(trifluoromethanesulfonyl)imide ( $\text{LiTFSI}$ ), lithium triflate ( $\text{LiTf}$ ), lithium hexafluoroarsenate ( $\text{LiAsF}_6$ ), and lithium tetrafluoroborate ( $\text{LiBF}_4$ ) [128]. Among these,  $\text{LiPF}_6$  is the most widely used commercial salt for LIBs. However,  $\text{LiTFSI}$  has been proposed for high-energy density LIBs, despite its potential to corrode current collectors at high voltages [129].

Electrolytes are categorized into various types based on the nature of solvents used, and their general properties are outlined in Table 5. The types of electrolytes include:

- (a) Aqueous electrolytes;
- (b) Non-aqueous electrolytes;
- (c) Ionic liquids;
- (d) Polymer electrolytes (gel polymer, solid polymer);
- (e) Hybrid electrolytes.

Furthermore, a brief comparison of their inherent properties is summarized in Table 6. Aqueous electrolytes have undergone modifications through several approaches, such as increasing salt concentration, incorporating additives, adjusting interfaces between electrodes, electrolytes, and current collectors, and developing new types such as gelled (hydrogel) and hybrid-solvent electrolytes. These modifications and their effects on different properties are detailed in Table 7. Aqueous electrolytes, with high wettability and improved interfacial kinetics, contribute to stabilizing the SEI layers, thus enhancing reversibility and providing thermodynamic stability to LIBs. Consequently, optimizing the potential window, increasing ionic conductivity, lowering the freezing point, and reducing costs are crucial for the development of promising hybrid electrolytes for LIBs.

**Table 5.** Types, advantages and disadvantages of various electrolytes used for LIBs.

Types	Advantages	Disadvantages	Refs
Aqueous	<ul style="list-style-type: none"> <li>Non-flammable</li> <li>Non-toxic</li> <li>High fluidity</li> <li>High dielectric constant</li> <li>High ionic conductivity</li> <li>Low cost</li> <li>Safe operation</li> <li>Long cycle life</li> </ul>	<ul style="list-style-type: none"> <li>Narrow potential window</li> <li>Low energy density</li> <li>Large overpotential</li> <li>Poor mechanical stability</li> </ul>	[130,131]
Non-aqueous	<ul style="list-style-type: none"> <li>Combination of cyclic and linear solvents enhance ionic conductivity and lower viscosity.</li> <li>Form stable SEI layer at the anode surface.</li> <li>Wide temperature range</li> <li>Wide potential window (~6.0 V)</li> <li>High energy density batteries</li> </ul>	<ul style="list-style-type: none"> <li>Poor ionic conductivity and low salts solubility</li> <li>High flammability and toxic reaction products</li> <li>Instability at high temperature and high current density</li> <li>Humid sensitive</li> <li>Thermal instability and high cost</li> <li>Extreme purification and handling</li> </ul>	[107,132,133]
Ionic Liquids	<ul style="list-style-type: none"> <li>Environment-friendly</li> <li>High chemical/thermal stability</li> <li>Tunable molecular structure</li> <li>High oxidation potential (~6.0 V)</li> <li>Zero vapor pressure</li> <li>Flame retardant</li> <li>Non-volatile</li> </ul>	<ul style="list-style-type: none"> <li>High viscosity</li> <li>Poor ionic conductivity</li> <li>Poor wettability</li> <li>Poor mechanical stability</li> <li>Large scale productivity</li> </ul>	[134–136]
Polymers (GPEs, SPEs)	<ul style="list-style-type: none"> <li>Low electrolyte leakage</li> <li>High flexibility</li> <li>Low flammability</li> <li>High stability</li> <li>No liquid solvents involvement</li> <li>Light weight</li> <li>Ease of processing</li> <li>Strong adhesion properties</li> <li>Large scale productivity</li> </ul>	<ul style="list-style-type: none"> <li>High viscosity</li> <li>Poor ionic conductivity</li> <li>Poor wettability</li> <li>Li+ ion transference number</li> <li>Moderate potential window (4.5 V~5.0 V)</li> </ul>	[106,107,137,138]
Hybrids	<ul style="list-style-type: none"> <li>Mechanical robustness</li> <li>Excellent processability</li> <li>Reduced interface resistance</li> </ul>	<ul style="list-style-type: none"> <li>Poor ionic conductivity</li> <li>Poor cation transference number</li> <li>Medium potential window</li> </ul>	[100,108,109]

**Table 6.** Summary of the inherent properties of various types of electrolytes used for LIBs.

Types	Aqueous	Non-Aqueous	Ionic Liquids	Polymer (Gels, Hybrid)
Mechanical strength	Poor	Good	Good	Medium
Ionic conductivity	$>10^{-3}$ Scm $^{-1}$	$>10^{-3}$ Scm $^{-1}$	$10^{-3} \sim 10^2$ Scm $^{-1}$	$>10^{-4}$ Scm $^{-1}$
Thermal stability	Poor	Medium	Good	Medium
Electrochemical stability	Poor	Good	Good	Poor
Safety	Poor	Medium	Medium	Medium
Interfacial properties	Good	Medium	Good	Medium

**Table 7.** Modification strategies and general properties of aqueous electrolytes used for LIBs.

Electrolytes	Strategies	General Properties	Refs
Aqueous	Enriching salt concentration	Cut anions at anode surface Enhance anion/cation interaction Break hydrogen bonding to reduce O <sub>2</sub> solubility and H <sub>2</sub> evolution Develop eutectic system for better ORR kinetics to improve the potential window (1.23 to ~3.0 V) Improve the ionic conductivity ( $\approx 10^2$ ) Affect the rate performance and overpotential Suppresses OER at the cathode surface Prevent corrosion/dendrite formation	[130,131,139]
	Incorporating additive	Modifies interfaces (electrodes/current collectors/electrolyte/separator) Change solvation sheath to widen potential window for high temperature and freezing temperature Suppresses free radicals, reactive anions/cations to control side reactions	[139]
	Tuning interfaces \ (electrodes/current collectors/electrolyte)	Affects interfaces stability and reactivity To achieve thermodynamics (chemical, thermal) and kinetic (charge/mass transportation activity) stability Solidifies water (lower fluidity)	[140,141]
	Addition of decoupling gel/polymer material	Develop anti-freezing function at low temperature Stabilize/widen the potential window and working temperature range Lowers the production cost Efficiently reduce the cost and environmental problems	[142,143]
	Solvent-hybrid electrolyte	Improve interfacial chemistry Enhance performance of LIBs	[144]

The non-aqueous electrolytes, typically comprising lithium salts and organic solvents (such as carbonates, acetals, ethers, esters, sulfones, sulfites, and sulfoxides), are designed to maintain desired conductivity, viscosity, and compatibility with battery components. Key parameters include ionic conductivity, viscosity (ideally  $< 2 \text{ mPa}\cdot\text{s}$ ), dielectric constant, wettability, working temperature range, flash point, and environmental impact [145]. Carbonates are commonly used due to their excellent electrochemical properties and ability to support a high-quality SEI layer, crucial for preventing dendrite formation and ensuring battery safety. For instance, ethylene carbonate (EC) is frequently employed in electrolytes like 1 M LiPF<sub>6</sub> in EC:DMC:DEC (1:1:1) and 1.2 M LiPF<sub>6</sub> in EC:EMC (3:7), which showed electrochemical stability windows of 4.5 V and 4.9 V, respectively [146,147]. Physicochemical and electrochemical properties of different organic solvents (carbonates, acetals, ethers, esters, sulfones, sulfites, and sulfoxides) are summarized in Table 8. Selecting solvents with high dielectric constants, low viscosity, and high ionic conductivity is essential for enhancing the electrolyte's oxidation potential and promoting electrocatalytic reactions, thereby improving the performance of high energy density LIBs [148].

**Table 8.** Physicochemical and electrochemical data of some organic solvents for non-aqueous electrolytes.

Solvents	Names	m.p	b.p	$\eta$ (20 °C)	$\epsilon_r$	$\mu$	$\rho$ (V <sub>m</sub> )	$\kappa$	E <sub>ox</sub> vs. Li <sup>+</sup> /Li	Ref
Carbonates	EC	36.4	248	1.90	89.8	4.61	1.32 (66.71)	8.3	6.7	[149]
	PC	-48.8	242	2.53	64.9	4.81	1.20 (85.08)	5.6	6.0	[150]
	DMC	4.6	96	0.59	3.1	0.76	1.06 (84.98)	6.0	5.5	[148]
	DEC	-74.3	126	0.75	2.8	0.96	0.97 (121.78)	2.4	5.2	[133]

**Table 8.** Cont.

Solvents	Names	m.p	b.p	$\eta$ (20 °C)	$\epsilon_r$	$\mu$	$\rho$ ( $V_m$ )	$\kappa$	$E_{ox}$ vs. $Li^+/Li$	Ref
Esters	EA	-84	77	0.45	6.0	1.83	0.90 (97.90)	11.5	5.4	[151]
	MA	-98.2	57	0.37	6.7	1.70	0.93 (79.66)	14.8	5.2	[152]
	MB	-84	102	0.60	5.5	1.71	0.90 (113.48)	4.2	4.6	[153]
	EPE	-126.7	63	0.31	-	1.16	0.73 (120.75)	4.5	5.5	[154]
Ethers/Acetals	DEE	-74	121	0.56	5.1	1.76	0.84 (140.69)	5.8	4.5	[155]
	THF	-109	66	0.46	7.4	1.70	0.88 (81.94)	9.1	3.5	[156]
	DMSO	18.5	189	1.90	46.6	3.90	1.09 (71.68)	8.6	4.1	[157]
Sulfur Compounds	DMS	-141	126	0.87	22.5	2.90	1.20 (91.78)	13.6	4.2	[158]
	DES	-112	156	0.83	15.6	2.96	1.08 (127.94)	10.2	2.9	[159]

Abbreviations: m.p = melting point, b.p = boiling point,  $\eta$  = dynamic viscosity in mPa,  $\epsilon_r$  = dielectric constant,  $\mu$  = dipole moment,  $\rho$  = density ( $\text{g}\cdot\text{cm}^{-3}$ ),  $V_m$  = molar volume ( $\text{cm}^3\cdot\text{mol}^{-1}$ ),  $\kappa$  = ionic conductivity of 1 M LiPF6 ( $\text{m}\cdot\text{Scm}^{-1}$ ),  $E_{ox}$  = oxidation potential. Chemical Name: EC = ethylene carbonate, PC = polycarbonate, DMC = dimethyl carbonate, DEC = diethyl carbonate, EA = ethyl acetate, MA = methyl acetate, MB = methyl butyrate, EPE = 3-(1,1,2,2-tetrafluoroethoxy)-1,1,2,2-tetrafluoropropane, DEE = 1,2-diethoxyethane, THF = tetrahydrofuran, DMSO = dimethyl sulfoxide, DMS = dimethyl sulfide, and DES = diethyl sulfite.

Ionic liquids (ILs) offer benefits such as flame retardancy, non-volatility, and thermal stability, but their high viscosity can reduce ionic conductivity and affect the rate-performance of lithium-ion batteries (LIBs). To address this, anti-freezing agents like acetonitrile or ethylene glycol are added to enhance dielectric constants, miscibility, and oxidation stability at lower temperatures [160]. Despite their advantages, ILs face challenges such as high viscosity and poor wettability with battery components, which limit their practical use. ILs are considered “green solvents” and are used to mitigate issues like volatility and low oxidation potential seen in traditional organic solvents [146,148,161]. They are composed of ionic bonds between cations and anions and can dissolve a variety of substances. Adding low-viscosity compounds can improve their ionic conductivity [134,136]. ILs are categorized into aprotic, protic, and zwitterionic types based on their chemical composition. Aprotic ILs, which lack free protons, are used as co-solvents, while protic ILs, which contain free protons, offer better ionic conductivity and are used in fuel cells and batteries [162]. However, ILs generally have high melting points and strong ionic bonds, leading to high viscosity and reduced ionic conductivity, which can hinder LIB performance [135]. To overcome these limitations, strategies such as blending ILs with organic solvents and modifying the cation side chains are being explored. These solutions, while improving performance, often increase costs and require extensive purification, limiting their commercialization in energy storage applications.

Polymer electrolytes (PEs) are emerging as a solution to the limitations of liquid electrolytes, such as leakage, poor volume suppression, and safety issues. PEs offer benefits including low leakage, high flexibility, low flammability, stability between electrolyte and electrodes, no liquid solvents, lightweight, easy processing, and strong adhesion. Also known as solid polymer electrolytes (SPEs), they consist of lithium metal salts dissolved in a polymer matrix. These can be classified into organic electrolytes with polymer composites and inorganic electrolytes with materials like ceramics and perovskites. While organic electrolytes often suffer from poor ionic conductivity, inorganic electrolytes face issues with mechanical stability and large-scale production. High ionic conductivity, large  $\text{Li}_+$  ion transference number, wide electrochemical stability window, high mechanical stability, low electrolyte/electrode impedance, electrical insulation, low cost, ease of manufacturing, sustainability, and environmental compatibility are the significant design parameters for polymer electrolytes. [163–165] Ionic conductivity can be improved by choosing suitable polymers (linear, branched, or crosslinked), adding new salts, and incorporating fillers. Common polymers used in PEs include PEO, poly (vinylidene fluoride; PVDF), poly (ethylene carbonate; PEC), poly (acrylonitrile; PAN), and poly (ethylene glycol; PEG) [166,167]. The size of the anionic component in lithium salts affects ionic conductivity; larger an-

ions increase ionic contact distance and dissociation, thus enhancing conductivity. The dissociation constants of commonly used salts can be explained in the following order: LiCF<sub>3</sub>SO<sub>3</sub> < LiBF<sub>4</sub> < LiClO<sub>4</sub> < LiPF<sub>6</sub> < LiAsF<sub>6</sub> < LiN (CF<sub>3</sub>SO<sub>2</sub>)<sub>2</sub> [161,168]. Fillers, both active (e.g., ionic liquids and lithium salts) and passive (e.g., carbonaceous compounds and ceramics), can improve the ionic conductivity, thermal stability, and mechanical properties of SPEs [137,169,170]. However, poor compatibility with separators and electrodes, along with a moderate potential window (4.5 V~5.0 V), limits their application in high voltage LIBs, necessitating further research for high-potential window polymer electrolytes.

Hybrid electrolytes (HEs) are an advanced research focus, combining polymer and inorganic/organic electrolytes to achieve mechanical robustness, high ionic conductivity, and reduced interfacial resistance. Despite these advantages, they generally exhibit lower ionic conductivity, a lower cation transference number, and a medium potential window. The properties of HEs, such as melting point, glass transition temperature, and crystallinity, are influenced by the molecular groups attached to the polymer chain, affecting their overall performance. HEs are classified into solid/liquid, solid/solid, or liquid/solid/liquid types, incorporating inorganic or organic compounds as fillers to modify the polymer matrix. The liquid electrolytes are organic or aqueous, whereas the solid electrolytes are polymers and LISICON [171–173]. While they combine characteristics of both polymers and other types of electrolytes, further research is needed to improve ion transport, interfacial properties, and potential window. New polymer matrices and fillers need to be designed and tested to enhance high-performance hybrid electrolytes [174,175]. For effective design, hybrid electrolytes must have high ionic conductivity, a wide electrochemical stability window, versatility across temperatures, good interfacial compatibility, high cation transference number, mechanical strength, low viscosity, high dielectric constants, and safety features such as non-flammability, non-toxicity, and eco-friendliness. These qualities are essential for developing high-power, high energy density LIBs.

The liquid electrolyte offers high ionic conductivity, good wettability, and superior interfacial contact, contributing to excellent electrochemical performance. However, its volatility and flammability pose safety risks, leading to irreversible active material loss during charge-discharge cycles. In contrast, solid-state electrolytes prevent the transfer of intermediate products, reducing the shuttle effect and lithium dendrite growth. They provide low flammability, high thermal stability, and no leakage, enhancing safety and battery lifespan. Solid-state electrolytes also minimize material usage, resulting in reduced mass and volume per capacity unit and enable the use of higher-capacity electrode materials, boosting energy density and safety [176]. Common solid-state electrolytes include oxide (e.g., garnet-type Li<sub>7</sub>La<sub>3</sub>Zr<sub>2</sub>O<sub>12</sub>) [177–180], sulfide (e.g., Li<sub>2</sub>S-SiS<sub>2</sub>) [181–183], and polymer electrolytes (e.g., PVDF) [184–186]. Oxide electrolytes achieve ionic conductivity of 10<sup>-4</sup> Scm<sup>-1</sup> at room temperature, while sulfide electrolytes can reach up to 10<sup>-3</sup> Scm<sup>-1</sup> due to their wider ion transport channels. Polymer electrolytes facilitate ion transport through Li<sup>+</sup> complexation, reducing reactivity with electrodes and enhancing safety. Xiong et al. reported that the mechanical failure of solid-state electrolytes in lithium metal batteries, driven by lithium anode growth, is linked to interfacial and internal defects [187,188]. A modified electro-chemo-mechanical model reveals how these defects influence stress transmission and damage propagation, providing insights for designing safer, high energy density solid-state batteries.

### 3.3. Design Parameters Directly Affecting Performance

Performance is a crucial metric for assessing the energy storage capability of LIBs, specifically their ability to endure electrochemical reactions over time under severe conditions. It encompasses a correlation among all design parameters, material selections, reaction kinetics, and thermodynamics. Reaction kinetics, in particular, explores the relationship between physicochemical and electrochemical reactions. The physicochemical reaction includes both physical properties such as surface area, porosity, density, wettability, conductivity, and thickness and chemical properties such as chemical potentials,

reactions, and thermodynamics. They together clarify the reaction kinetics at the interfaces among electrodes, electrolytes, and current collectors, as well as the transportation of ions within the electrolyte (refer to Figure 6). Electrochemical reaction kinetics, on the other hand, focus on the ion/charge transportation mechanism during the chemical reactions within the electrolyte throughout the charge and discharge processes. The relationship between various physicochemical and electrochemical properties defines key critical design parameters, such as conductivity, electrochemical potential window, reaction chemistry, and thermodynamics of LIBs. Optimizing these design parameters is essential for achieving optimal performance that meets industrial energy consumption demands.

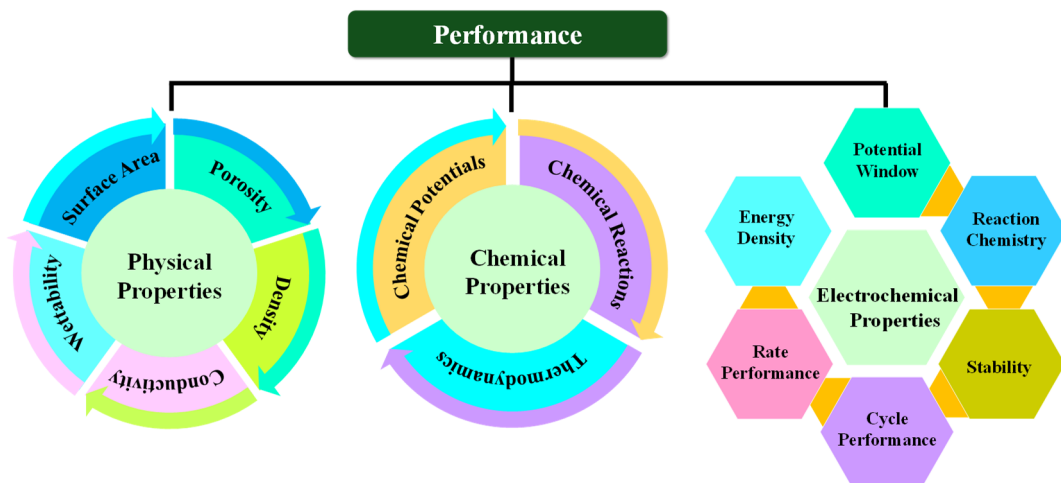


**Figure 6.** Substantial properties influencing the overall performance of full-cell LIBs.

### 3.3.1. Conductivity

Both electronic and ionic conductivities are intrinsic performances that play a crucial role in determining the flow of electrons and ions within the electrodes. They can be extrinsically modified to improve the capacity, cyclability, and rate performance of LIBs. The electrical conductivity depends mainly on the electronic structure of electrode materials. The electronic structure has multiple electrons in the valence band with the minimum energy band gap to increase electrical conductivity. Materials such as metalloids, post-transition metals, and some reactive nonmetals exhibit higher electrical conductivity compared to transition metals and their oxides. Several methods have been employed to enhance electrical conductivity, such as introducing point defects in the crystal structure, doping with other elements, forming composites, surface etching, and coating materials with metals, metal oxides, or carbonaceous compounds [189–193]. For instance, doping metal elements into electrode materials can increase electrical conductivity by up to  $10^3$  times, while coating with carbonaceous or metal oxide layers can reduce the energy band gap and improve conductivity. Enhancing electrical conductivity lowers charge transfer resistance and boosts the specific capacity and energy density of LIBs. A recent study demonstrated that developing an eco-friendly carbon composite made from microalgae combined with an  $\text{SnO}_2$  anode led to increased reversible capacity, improved cycle stability, and mitigation of volume expansion issues in LIBs [60]. Additionally, coating CN-LTO using a chemical reflux technique increased the electrical conductivity of pristine LTO from  $1.58 \times 10^{-9}$  to  $4.29 \times 10^{-6} \text{ S/cm}$  [194].

Ionic conductivity, which governs ion transport mechanisms, is another factor influencing the rate performance and power density of LIBs. It can be improved by modifying the morphology, particle size, and physicochemical properties of the electrode materials, electrolyte, separators, and binders, which in turn affect the adsorption and diffusion behavior at electrode surfaces. In particular, nanomaterials significantly reduce the diffusion length of  $\text{Li}^+$  ions and enhance their diffusivity. The residence time ( $\tau$ ) is the duration for which  $\text{Li}^+$  ions remain within the electrode, while diffusion length ( $L$ ) describes the length

of the diffusion pathway through the crystal structure of the electrode. They are related through the diffusivity ( $D$ ) as follows:

$$\tau = \frac{L^2}{D} \quad (6)$$

Moreover, ionic conductivity is related to porosity and tortuosity of electrodes and separators. Porous structures in electrodes and separators provide extensive diffusion pathways, facilitating faster diffusion of  $\text{Li}^+$  ions, reducing charging time, and enabling rapid charging in LIBs. Tortuosity, the complexity and geometry of the surfaces, offers multiple diffusion channels that enhance the movement of  $\text{Li}^+$  ions. Voids and pores, formed by particle interactions and distances, play a crucial role in electrolyte penetration, thereby increasing the diffusion of  $\text{Li}^+$  ions. Moreover, the surface area of the electrode materials significantly affects the adsorption kinetics of  $\text{Li}^+$  ions, as well as the behavior of redox couples and free radicals generated during electrochemical reactions. A high surface area allows for more active sites for  $\text{Li}^+$  ion adsorption and promotes better electrolyte penetration, facilitating improved  $\text{Li}^+$  ion diffusion during electrochemical reactions, which is essential for achieving high specific capacity and energy density.

The cationic transference number, affecting the rate performance and power density of LIBs, is another critical factor, particularly in selecting appropriate electrolytes to enhance conductivity. Therefore, it is necessary to identify electrode materials with high porosity, appropriate tortuosity, many voids, and a substantial specific surface area to optimize  $\text{Li}^+$  ion diffusion and reduce the charging times of LIBs. Furthermore, it is advisable to use electrolytes with high conductivity and an optimized cationic transference number to improve rate performance, ensure electrochemical potential stability, and enhance specific capacity, cycle life, and safety. In addition, separators must be porous to maintain open pores and prevent the formation of lithium dendrites, which can cause internal short circuits and thermal runaway. Consequently, the careful design and optimization of both electrical and ionic conductivity are vital for enhancing the overall performance of full-cell LIBs.

### 3.3.2. Electrochemical Potential Window

An electrochemical potential window is a design parameter that determines the range within which various electrochemical reactions can occur, directly impacting the performance of a full-cell LIB. It is influenced by the standard redox potentials of electrodes, electrolytes, separators, binders, and current collectors versus the standard hydrogen potential (SHE) [195]. The difference in potentials between cathode and anode in the absence of applied current is called electromotive force (EMF) or open-circuit voltage (OCV) of the LIBs and is determined by the nature of electrode materials. The voltage potential  $V_{\text{OC}}(\phi)$  is determined by the Nernst equation given below:

$$V_{\text{OC}}(\phi) = -\Delta F_F = -\left(\frac{\mu_C - \mu_A}{F}\right) \quad (7)$$

where  $F$  is the Faraday constant, and  $\mu_C$  and  $\mu_A$  are the chemical potentials of cathode and anode materials in full-cell LIBs, respectively [196,197]. The energy band gap between the highest occupied molecular orbital (HOMO) and the lowest unoccupied molecular orbital (LUMO) of the electrolyte determines the voltage potential. The energy band gap between the highest occupied molecular orbital (HOMO) and the lowest unoccupied molecular orbital (LUMO) of the electrolyte determines the voltage potential of a full-cell LIB. For optimal performance, the chemical potential of the cathode material should be above the HOMO, while that of the anode should be below the LUMO of the electrolyte, as shown in Figure 7 [198]. This arrangement ensures a stable electrochemical environment, minimizing undesirable reactions and improving the overall voltage stability and efficiency of the LIBs.

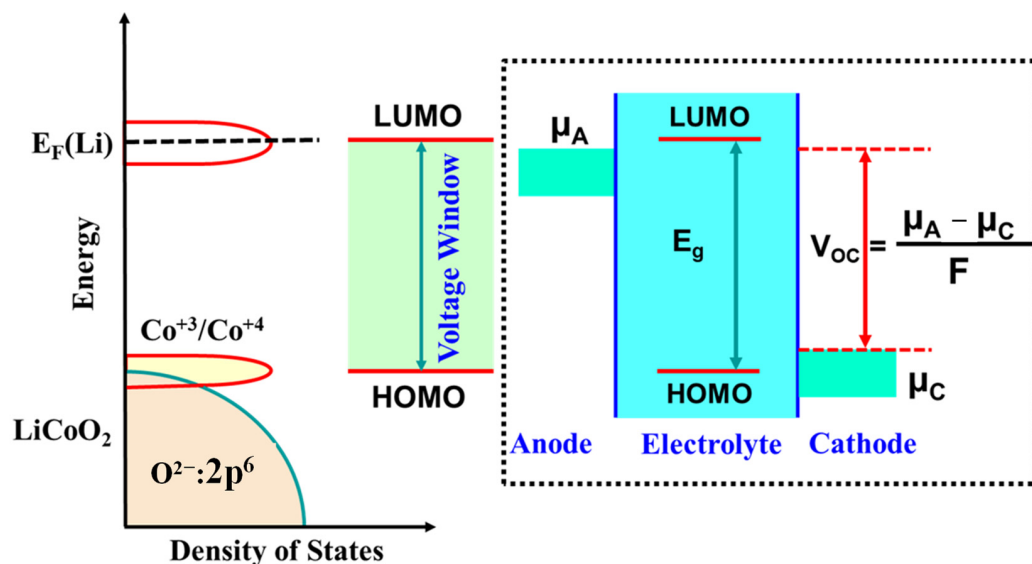


**Figure 7.** Energy phases of electrochemical potentials of Li metal and  $\text{LiCoO}_2$ , and their respective HOMO and LUMO energy positions in electrolytes. (Dotted Box) Relative energy of electrolyte, and HOMO and LUMO positions of electrolytes and electrodes.

In addition, electronegativity, the ability of an atom or a functional group to attract electrons, plays a crucial role in determining the electrochemical potential of electrode materials. The higher the electronegativity of an atom or functional group, the greater its oxidation potential. Obviously, fluorine and oxygen atoms are commonly used in the development of cathode materials for LIBs. Conversely, atoms or functional groups with lower electronegativities possess low reduction potentials, making them suitable for constructing anode materials. A functional group with high oxidation potential and low reduction potential creates electrodes with a high potential difference, leading to high energy density [199]. The potential difference between electrodes is influenced by the nature of polyanionic groups and the percentage of ionic bonding between cations and anions. Replacing oxygen atoms in polyanionic groups with fluorine increases the ionic bond characteristics, resulting in a larger potential difference. For example, transition metal phosphates, silicates, and sulfates exhibit higher potential differences compared to oxygen-based compounds [200].

Another crucial factor affecting the potential difference is the occupation of different lattice sites by various atoms, each corresponding to a distinct energy level and crystal structure. The insertion and extraction of  $\text{Li}^+$  ions and corresponding electrons from the 3D orbitals of transition metals alter the crystal structure or cause phase transformations. The energy required for these processes correlates with the electrochemical potential of the LIBs [201]. Lattice energy, the enthalpy change ( $\Delta H$ ) involved in the  $\text{Li}^+$  ion intercalation process, affects the Gibbs free energy ( $\Delta G$ ), which ultimately determines the electrochemical potential of the battery [202,203]. Crystal defects, such as the substitution of foreign atoms or ions in place of inherent lattice atoms, cause lattice distortion, altering the lattice energy and influencing both the electrochemical potential and thermal properties of electrode materials [204]. The electronic structure, which defines the number of electrons inserted or extracted during oxidation and reduction reactions, also correlates with the electrochemical potential. Changes in crystal and electronic structures can cause phase transformations, contributing to changes in enthalpy and Gibbs free energy ( $\Delta G$ ) [201]. Thus, it is essential to consider the electronegativity of atoms, the nature of chemical bonds (describing polyanionic groups), crystal structures, lattice energy, crystal defects, and electronic structures of both electrodes and electrolytes to design a stable and wide electrochemical potential window for full-cell LIBs.

### 3.3.3. Electrochemical Reaction Kinetics

The electrochemical reaction mechanism is a key determinant of the redox behavior of electrodes and their overall performance in LIBs. This mechanism is influenced by several factors, including the nature of the electrode materials, their crystal and electronic structures, the properties of the electrolyte, and the electrochemical potential window. Based on the characteristics of lithiation and de-lithiation processes, electrochemical reaction mechanisms are generally categorized into intercalation/de-intercalation, alloy/de-alloy, conversion, and mixed-type reactions. Each type of reaction has its own fundamental issues and theoretical specific capacity range, as illustrated in Figure 8. These mechanisms play a pivotal role in dictating the efficiency, stability, and specific capacity of the electrodes, with each presenting its own set of challenges and advantages. Understanding and optimizing these mechanisms is crucial for the development of high-performance LIBs.

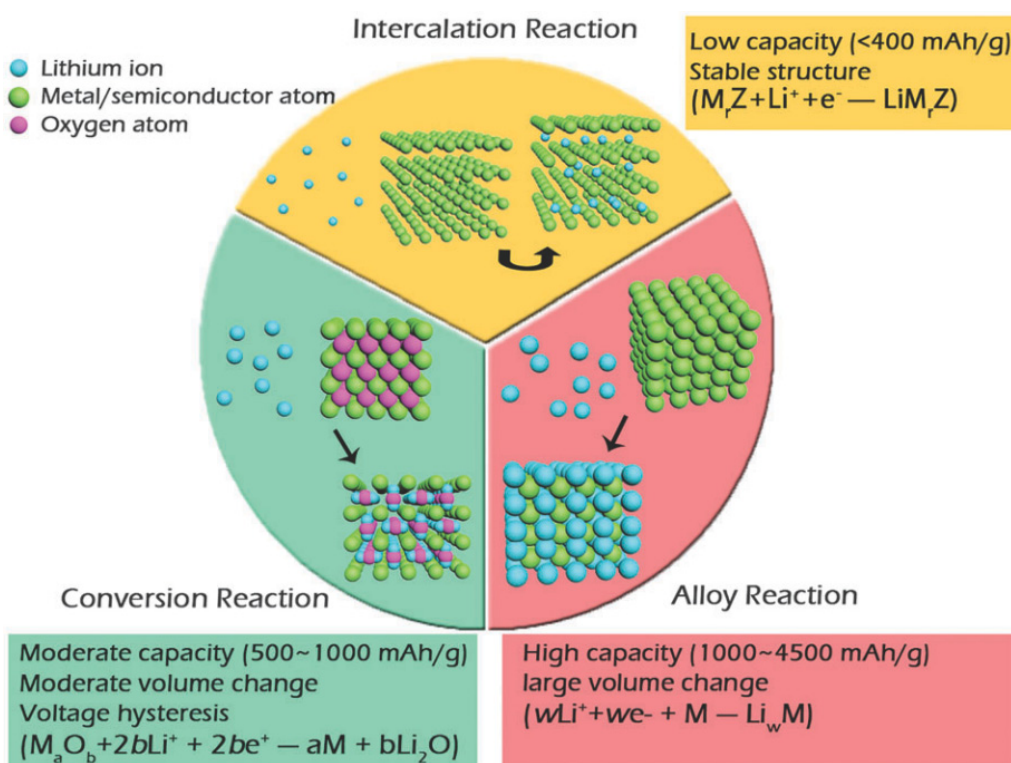
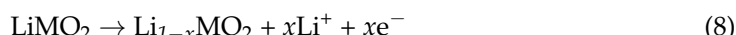
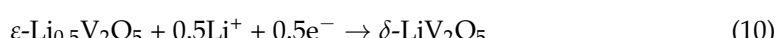


**Figure 8.** Illustration of fundamental electrochemical reaction mechanisms for LIBs (Reprinted/adapted with permission from Ref. [205] published by Royal Society of Chemistry, 2015).

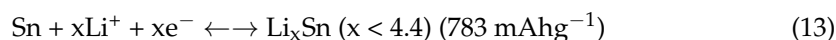
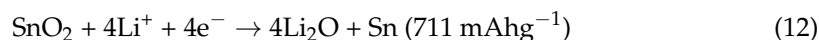
The movement of  $\text{Li}^+$  ions between cathode and anode, known as intercalation/de-intercalation mechanism, is the foundational electrochemical reaction mechanism in LIBs. It is explained as follows:



Nevertheless, some electrode materials undergo phase transition during this process, which can hinder the electrochemical process and restrict the electrochemical activity of LIBs. For example,  $\text{V}_2\text{O}_5$  cathode material undergoes various phase transformations during lithiation, as expressed by Refs [76,205].



The intercalation/de-intercalation process maintains the system's thermal stability by preserving structural integrity and limiting the evolution of gases such as H<sub>2</sub> and O<sub>2</sub>, making it suitable for long-life LIBs. Anode materials like carbon compounds and titanium oxides are preferred for LIBs because they follow this mechanism. For cathode materials, oxides of vanadium (e.g., V<sub>2</sub>O<sub>5</sub>, VO<sub>2</sub>, LiV<sub>3</sub>O<sub>8</sub>), spinel oxides (e.g., LiM<sub>2</sub>O<sub>4</sub> where M = Mn, Co, Ni), polyanionic oxides (e.g., LiMPO<sub>4</sub> where M = Fe, Mn, Co, Ni), and certain layered oxides (e.g., LiMO<sub>2</sub> where M = Co, Mn, Ni, including NCM variants such as 811, 622, 333) are prominent choices. However, electrodes using the intercalation/de-intercalation mechanism often suffer from poor intrinsic conductivity, limited specific capacity, and potential hysteresis. To address these issues, the alloy/de-alloy reaction mechanism has been developed. Metal electrodes such as Si, Sb, Zn, and Sn, which follow the alloy/de-alloy reaction, offer high specific capacities, high-rate performance, and high energy density. With the exception of Ge and Sb, these metals are characterized by high electrical conductivity, abundance, low cost, and non-toxicity. They form distinct lithium alloys until the lower cut-off voltage of LIBs. Therefore, it is crucial to investigate the distinct phases of lithium alloys and the number of moles of Li<sup>+</sup> ions involved in the alloy/de-alloy reaction [19]. For example, SnO<sub>2</sub> nanoparticles encapsulated in a mesoporous carbon composite (SnO<sub>2</sub>@MPC) anode form lithium alloys with distinct phases under several steps as follows:

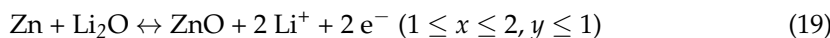
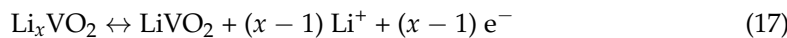
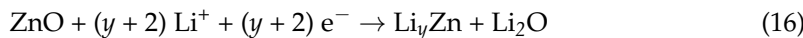
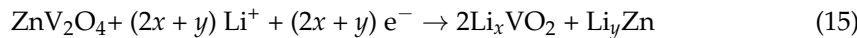


The alloy/de-alloy reaction in LIBs often results in an unstable SEI layer during charge and discharge cycles. This reaction is characterized by significant volume expansion and contraction—up to ~300% for Si anodes—far exceeding the ~150% expansion seen with intercalation/de-intercalation mechanisms [60]. These large volume changes lead to severe issues such as substantial capacity fading, poor rate performance, sluggish reaction kinetics, and structural instability [48,49]. In contrast, the conversion reaction involves transforming the electrode material into its constituent or derivative compounds. For example, the formation of Li<sub>2</sub>O has been observed with N-doped reduced graphene oxide (rGO) wrapped around Mn<sub>2</sub>O<sub>3</sub> nanorods, along with the conversion of MnO and Mn [206]. It addresses major issues such as poor specific capacity and environmental concerns, offering excellent rate performance and high energy density for LIBs. This improvement is demonstrated by the following general electrochemical reaction:



where 'X' is any of chalcogenides such as oxides, sulfides, nitrides, carbides, etc. Common materials used as anode materials for LIBs in the conversion-type reaction mechanism include 3D-transition metal oxides such as CuO, NiO, and M'<sub>2</sub>O<sub>3</sub>/M'<sub>3</sub>O<sub>4</sub> (M' = V, Mn, Fe, Co, and Ni), as well as binary oxides like ferrites, manganites, and cobaltites (M'M''<sub>2</sub>O<sub>4</sub>, where M'/M'' = Ni, Zn, Fe, and Co). These materials typically exhibit potential stability windows around ~3.0 V vs. Li/Li<sup>+</sup>, deliver high specific capacities (~700 mAhg<sup>-1</sup>), and are suitable for high energy density LIBs. However, they encounter significant challenges, including large potential hysteresis, capacity fading, poor intrinsic conductivities, and irreversible capacity loss [207]. To address these issues, a new electrochemical reaction mechanism known as the mixed reaction mechanism has been developed. This mechanism involves lithium insertion/extraction combined with alloy/de-alloy or conversion reactions. Vanadium-based binary oxides such as MV<sub>2</sub>O<sub>4</sub>/M<sub>2</sub>VO<sub>4</sub>, MV<sub>2</sub>O<sub>6</sub>, MV<sub>2</sub>O<sub>7</sub>, and M<sub>3</sub>V<sub>2</sub>O<sub>8</sub> (where M = Ni, Zn, Co, Mn, and Fe) are used in this mixed reaction mechanism. For instance, Zn-based vanadium metal oxides undergo alloy/de-alloy reactions upon lithiation, leading to the formation of a vanadium-based matrix that follows the insertion/extraction reaction mechanism, while Zn metal/metal oxides participate in the alloy/de-alloy reaction. For example, ZnV<sub>2</sub>O<sub>4</sub> converts into ZnO and a lithiated vanadium oxide matrix (Li<sub>y</sub>VO<sub>2</sub>). During the charge/discharge process of LIBs, these components

separately and spontaneously undergo alloy/de-alloy ( $\text{Li}_x\text{Zn}$ ) and insertion/extraction reactions as follows:



Transition metals based on vanadium oxides typically follow conversion and insertion/extraction reaction mechanisms. For instance,  $\text{Ni}_3\text{V}_2\text{O}_8$  hollow microspheres convert into  $\text{NiO}/\text{Ni}$  metal and a lithiated vanadium oxide matrix ( $\text{Li}_{x}\text{V}_2\text{O}_5$ ), delivering a high specific capacity [208]. The excellent rate performance of these materials for LIBs is attributed to the in situ formation of metal/metal oxide layers during the mixed electrochemical reaction mechanism. This process enhances thermal stability, minimizes irreversible capacity loss and volume changes, and improves conductivity due to the electroactively lithiated vanadium oxide matrix. Consequently, intercalation and mixed electrochemical reactions are considered the most desirable mechanisms for the development of high energy density LIBs.

### 3.3.4. Efficiency

The efficiency, the ratio between output energy to input energy for a full-cell LIBs, measures the battery's ability to deliver a specific amount of energy for applications such as smartphones, laptops, and tablets. It is described in terms of coulombic efficiency and energy efficiency as follows:

$$\text{Coulombic Efficiency}(\%) = \frac{\text{Total Discharge Capacity}}{\text{Toal Charge Capacity}} \times 100 \quad (20)$$

$$\text{Energy Efficiency}(\%) = \frac{\text{Discharge Energy Density}}{\text{Charge Energy Density}} \times 100 \quad (21)$$

Coulombic efficiency refers to the proportion of  $\text{Li}^+$  ions effectively cycled within a full-cell LIB, comparing the amount of  $\text{Li}^+$  ions extracted from the cathode to those inserted into the anode during cycling. It represents the ratio of the obtained specific capacity to the amount of  $\text{Li}^+$  ions cycled. Ideally, if the same amount of  $\text{Li}^+$  ions is extracted and inserted, coulombic efficiency would be 100%. However, practical observations show that some  $\text{Li}^+$  ions are not fully recovered due to factors like SEI layer formation and electrode material characteristics. For instance,  $\text{LiCoO}_2$  might deliver a certain number of Li atoms to reach a fully charged state ( $\text{Li}_{0.5}\text{CoO}_2$ ) but only recover a reduced amount ( $0.9 \times$  number of Li atoms), leading to a coulombic efficiency of around 90%.

Energy efficiency, on the other hand, pertains to the overpotential of the LIB. Each electrode has a different redox potential, and Li atoms require varying amounts of energy for insertion or extraction. If some Li atoms are extracted at 2.0 V while others require 4.0 V during charging, the energy used to insert or extract these atoms differs, indicating large overpotentials that cannot be recovered. Thus, energy efficiency is determined by the discharge/charge curves of the LIBs, where each point on the curve represents the energy required for the insertion or extraction of Li atoms. The height of these profiles, alongside the length of the x-axis, is crucial for assessing the energy efficiency of the LIB. Both the nature of the electrodes, including their physicochemical properties, particle sizes, and electrochemical reaction kinetics, play significant roles in defining the efficiency of full-cell LIBs.

### 3.4. Productivity and Cost of Full-Cell LIBs

The cost and weight of a full-cell LIB are influenced by the selection of materials, the fabrication process, and the desired dimensions, which are determined based on the intended application. We primarily focused on coin-type full cells with CR2032 dimensions for simplicity. The weight of a coin cell is determined by several components: current collectors (aluminum and copper foils), reference electrodes (lithium foil), the amount of electrolyte, the mass loading of electrode materials (both anode and cathode), and additional winding components such as wave springs, gaskets, casings, spacers, and separators. The mass loading and weight of the electrodes need to be controlled during fabrication. The active mass of the electrodes is determined by the proper mixing of carbon additives and polymer binders with the active material to produce the final electrodes. Variations in the mixing ratios (e.g., 60:20:20, 70:20:10, and 80:5:5) affect the final weight of the electrodes in the coin cell. The total weight of the coin cell is composed of 25.5% cathode material, 14.5% anode material, 6.9% aluminum current collector, 8.1% copper current collector, 11.2% electrolyte, 3.6% separator, and 30.2% battery casing, as depicted in Figure 9 [209]. Likewise, the cost of a full coin cell is dependent on the cost of each cell component, including spacers, gaskets, wave springs, casings, production line equipment (e.g., mixing machines, roller presses, electrode and electrolyte materials, and electrode cutters), lithium foil, current collectors, and the coin cell assembly environment, such as an argon-filled glove box. Therefore, optimizing the performance of the full coin cell LIBs is essential for determining its overall cost and achieving high energy density LIBs.

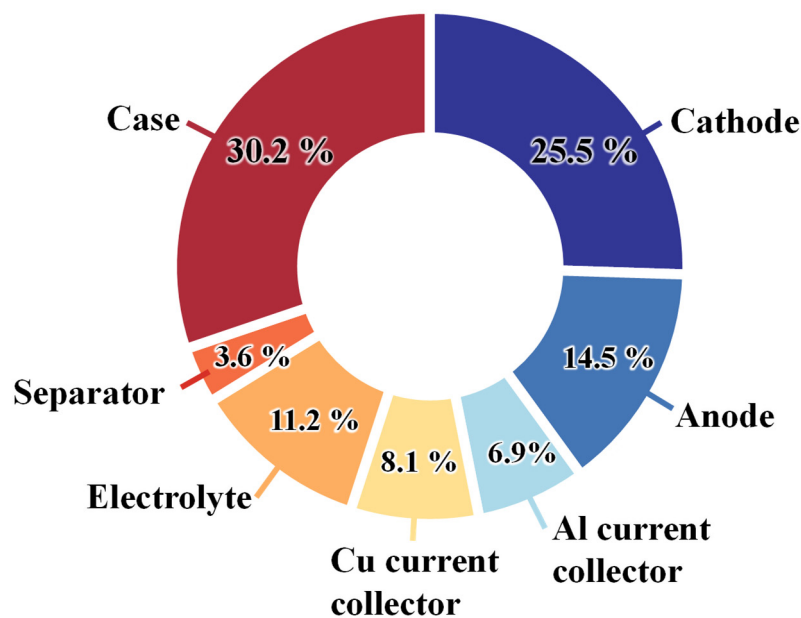


**Figure 9.** Weight percentage of main components of full-cell LIBs (re-drawn from the data from Ref. [209]).

#### 3.4.1. Cell Fabrication Processes

The cell manufacturing process plays a crucial role in determining various parameters such as electrode weight, thickness, porosity, tortuosity, mixing ratio, slurry rheology, and granule characteristics, all of which impact the potential window and performance of LIBs [210]. The manufacturing of electrodes typically involves a two-step process: slurry preparation and film formation, as shown in Figure 10 [211]. This process encompasses the entire sequence from active material mixing to slurry coating, solvent evaporation (drying), and further processing, such as calendaring, cutting, notching, etc. [104].

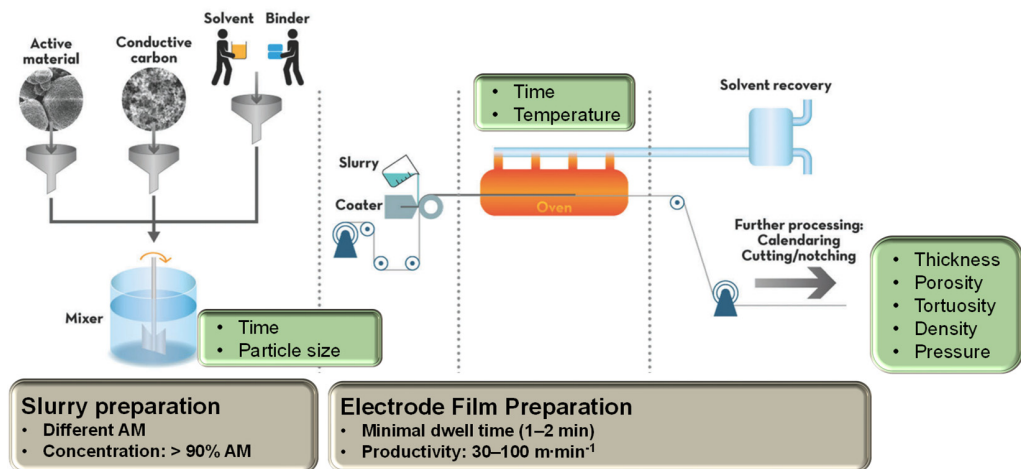


**Figure 10.** The manufacturing process of electrodes for full-cell LIBs along with main steps with most influential parameters. Adapted from Ref. [104] and modified.

Slurry preparation involves mixing active materials, carbon additives, and binders. Key factors include mixing time, particle size, chemical characteristics, and the choice of solvent. The mixing ratio of active materials with carbon additives and binders, along with the uniformity of granules and slurry rheology, directly affects the quality of the electrode film. A homogeneous slurry with minimal agglomeration and sedimentation ensures stable particle–solvent interactions, impacting viscosity and stability. At the laboratory level, proper particle dispersion and uniform mixing can be achieved through manual grinding with a mortar and pestle, ball milling, ultrasonic grinding, or magnetic stirring. In industrial sectors, methods such as ball milling, planetary mixing, high-speed mixers, hydrodynamic shear mixing, and homogenizers are used to achieve optimal particle dispersion and mixing [212]. The choice of solvent is crucial for determining the dispersibility and wettability of the slurry used in electrode manufacturing. The contact angle describes how well the solid particles interact with the solvent in the slurry. Key factors such as mixing time and the appropriate amount of solvent are vital for achieving uniformity and the desired rheological properties of the slurry. Extended mixing may improve the uniformity of the slurry's rheology but can lead to solvent evaporation. For instance, mixing carbon additives into the binder enhances mechanical and cohesive properties, forming an electronic network within the binder. However, this can make it challenging to achieve uniform mixing with active materials, potentially suppressing volume expansion, providing thermal/mechanical stability, and increasing irreversible capacity loss. On the other hand, when carbon additives are uniformly mixed with active materials, they cover the surfaces of active particles, enhancing the electron conductive network, improving conductivity, and potentially increasing specific capacity and energy density, although it may lead to slurry detachment from the current collector during the charging process.

The film preparation process involves spreading the slurry over the current collector, followed by drying to evaporate the solvent, and calendaring to optimize the thickness, porosity, tortuosity, and density of the film. The electrode thickness is controlled by the slurry spreading process, which can be performed using methods such as doctor blade coating in academic sectors or electrostatic deposition, roll coating, slot-die coating, and screen printing in industrial sectors [213,214]. The solvent evaporation is managed by drying the slurry at specific temperatures, times, and under vacuum conditions to ensure good adhesion and mechanical strength without cracking [215]. The calendaring process reduces electrode thickness and porosity, optimizing electrode density and affecting the wettability of the electrolyte and the overall performance of the full-cell LIBs [216,217].

In cell assembly, electrodes and separators are cut or slit to specific dimensions, stacked and wound together with the required amount of electrolyte before being packed using a punching machine. The dimensions of the LIBs are determined during the cutting/slitting

process, and electrolyte filling creates the necessary environment for the electrochemical reactions. Proper stacking and winding are essential to prevent gas leakage ( $O_2/H_2$ ), avoid component disintegration, and ensure mechanical stability. This delicate assembly process is typically conducted in an argon-filled glove box to maintain a dirt- and moisture-free environment. Finally, cell aging and inspection involve two stages: calendar aging and cycle aging. Calendar aging assesses capacity loss over time, while cycle aging measures capacity fading due to factors like voltage range, operating temperature, and charging rate [210,218]. The efficiency of the full-cell LIB is analyzed by charging and discharging cells under constant current (CC) and constant voltage (CV) phases for a specified number of cycles. Specific capacity, energy density, power density, efficiency, and charge/discharge times are determined, with specific C-rates correlating to the inspection time. The test scheme must specify the working voltage window, C-rate, weight, and thickness of electrodes to accurately determine the lifespan of the LIBs.

### 3.4.2. Mass Loading of Active Material

The specific capacity, energy density, overall cell packaging weight, and cell performance of LIBs are determined by the N/P ratio, which is defined as the ratio of the active mass loading amounts of negative (anode) to positive (cathode) electrode materials:

$$\text{N/P ratio} = \frac{\text{Mass of anode material}}{\text{Mass of cathode material}} \quad (22)$$

Higher or lower mass loading leads to poor specific capacity and hinder charge transportation. The mass loading amount is crucial for balancing the capacity of a full-cell LIB and is adjusted through the thickness of the electrode materials during film fabrication.

The anode materials such as Li metal ( $3860 \text{ mAhg}^{-1}$ ), graphite ( $372 \text{ mAhg}^{-1}$ ), silicon ( $4200 \text{ mAhg}^{-1}$ ), and SnO ( $782 \text{ mAhg}^{-1}$ ) deliver higher theoretical specific capacities than those of cathode materials, such as NCM811 ( $220 \text{ mAhg}^{-1}$ ), LiCoO<sub>2</sub> ( $140 \text{ mAhg}^{-1}$ ), LiMn<sub>2</sub>O<sub>4</sub> ( $148 \text{ mAhg}^{-1}$ ), LiFePO<sub>4</sub> ( $170 \text{ mAhg}^{-1}$ ), and LiV<sub>3</sub>O<sub>8</sub> ( $280 \text{ mAhg}^{-1}$ ) [219–222]. To achieve higher capacity and energy density in LIBs, the specific capacities should be considered based on nearly twice the mass loading amount of cathode materials. An anode-free configuration (0 N/P ratio) indicates no extra lithium is involved, which helps extend the life of LIBs. Thus, the recommended N/P ratio for full-cell configurations typically ranges between 1 and 1.2 [223]. The N/P ratio can be adjusted by varying the density of the anode materials. Increasing the N/P ratio generally reduces initial coulombic efficiency and increases the electrochemical potential of the anode material at the end of charge. This, in turn, can degrade the specific capacity and cycle life of the LIB. Research on different N/P ratios (1.10, 1.20, and 1.30) at room temperature ( $25^\circ\text{C}$ ) and a C-rate of 0.85C shows that cells with an N/P ratio higher than 1.10 suppress Li plating, while an N/P ratio of 1.20 enhances cycle life [224]. The impact of different N/P ratios (1.02, 1.06, 1.10, and 1.14) on the electrochemical performance of LiFePO<sub>4</sub> batteries at various temperatures ( $0^\circ\text{C}$ ,  $45^\circ\text{C}$ ) indicates that higher N/P ratios (1.10 and 1.14) provide better capacity retention compared to lower ratios [225]. Additionally, studies with different current collectors (Al and C) and mass loadings ( $1, 4 \text{ mg cm}^{-2}$  and  $1, 4, 8 \text{ mg/cm}^{-2}$ ) for LiAl<sub>0.1</sub>Mn<sub>1.9</sub>O<sub>4</sub> cathodes demonstrate that although high mass loading reduces specific capacities, it significantly improves capacity retention. Carbon-based current collectors showed higher specific capacity and retention compared to aluminum-based ones [226]. The tap density of materials affects LIB performance as it regulates the total mass per unit volume. The N/P ratio is influenced by the amount of active mass loading, which determines the utility of electrode materials during cycling. The diameter and thickness of materials also play a role; for example, a CR2032-sized coin cell LIB typically has an anode diameter of 10–12 mm and a cathode diameter of 12–14 mm. Using a smaller diameter for the anode plate helps adjust the utility of anode and cathode materials and minimize waste during cycling. Optimizing the N/P ratio is crucial for fabricating high energy density LIBs in a full coin cell configuration.

#### 4. Summary and Outlook

LIBs are prominent energy storage devices to meet the growing energy demands of the modern era. They offer high specific capacity, energy density, thermal stability, and long calendar life compared to other types of batteries. LIBs are used in a diverse range of applications, from powering household appliances to supporting electric vehicles. Effective LIB design must accommodate a significant number of  $\text{Li}^+$  ions while maintaining structural integrity, thermal and mechanical stability, and an optimal balance between energy and power density. This requires careful consideration of electrochemical reaction mechanisms. The design of LIBs involves numerous parameters that collectively impact their overall performance. This review aimed to detail key design parameters, their modification strategies, and their effects on the electrochemical performance of LIBs and reached the following summary.

- The full-cell configuration of LIBs includes electrodes (cathodes, anodes), current collectors, a separator, and an electrolyte. The cathode functions as the positive electrode with a high oxidation potential, facilitating the delivery of  $\text{Li}^+$  ions to the battery system. On the other hand, the anode acts as the negative electrode with a low reduction potential, accepting incoming  $\text{Li}^+$  ions. Current collectors are typically metal foils, metal oxides, or carbon fibers. Commonly used commercial current collectors include copper and aluminum foils. PP sheets, glass fibers, and sodium alginates are commonly used separators that prevent the flow of electrons while allowing the conduction of  $\text{Li}^+$  ions within the electrolyte. The electrolyte manages the transportation of  $\text{Li}^+$  ions and supports the chemical reactions. The electrolyte is a mixture of lithium salts ( $\text{LiClO}_4$ ,  $\text{LiPF}_6$ ,  $\text{LiTFSI}$ ,  $\text{LiTf}$ ,  $\text{LiAsF}_6$ ,  $\text{LiBF}_4$ ) and solvents (aqueous solutions, organic solvents, ionic liquids, polymers, and gels). A commercially used electrolyte is 1.0 M  $\text{LiPF}_6$  in a solvent mixture of ethylene carbonate (EC) and diethyl carbonate (DEC) at a 1:1 volume ratio, or in EC and dimethyl carbonate (DMC) at a 3:7 volume ratio.
- The design of full-cell LIBs involves several critical factors, including form factors (such as length, width, height, shape, and volume), material selection, performance, and productivity/cost aspects. Obviously, the form factors must be carefully considered to meet the requirements of LIBs. Material selection is most fundamental and crucial since it defines the electrochemical reaction mechanism, performance, and cost of LIBs. Designing electrode materials requires careful consideration of both intrinsic and extrinsic approaches. Binders should be designed with robust adhesion and cohesion properties, optimal binder selection, excellent distribution, free radical quenching capabilities, strong chelation, and electrochemical compatibility. Current collectors are evaluated based on electrochemical stability, density, mechanical strength, electrical conductivity, sustainability, and cost. Separators should be designed with attention to thickness, porosity, mean pore size (typically less than 1  $\mu\text{m}$ ), pore morphology, wettability, thermal stability, and mechanical properties. The development of electrolytes involves considering characteristics such as ionic conductivity, wide potential stability window, temperature tolerance, mechanical and thermal stability, chemical stability, and the ability to support the reaction kinetics of LIBs.
- Performance in full-cell LIBs is determined by several factors: conductivity, electrochemical reaction mechanisms, voltage window, efficiency, and thermodynamics. Both electrical and ionic conductivities significantly impact the specific capacity, energy density, power density, and cycle stability of LIBs. Electrical conductivity is governed by the electronic structure of the electrode materials, whereas ionic conductivity is influenced by the crystal structure, physicochemical properties, morphology, and particle size of the electrode materials, as well as the porosity and geometry of the separator. These factors directly or indirectly influence  $\text{Li}^+$  ion diffusion, which in turn affects the rate performance and power density of LIBs. Thus, a thorough investigation is necessary to evaluate the performance of LIBs. The potential window indicates the range of electrochemical reactions that can occur within HOMO and LUMO of

the electrolyte. It is influenced by factors such as the electronegativity of atoms, the nature of chemical bonds, lattice energy, crystal defects, and the crystal and electronic structures of both electrodes and electrolytes.

- Productivity is determined by factors such as the electrode fabrication process, mass loading amount, and processability, all of which impact the cost and weight of the final product. Key factors influencing the final electrode's properties include process parameters that affect the compact density, thickness, mass loading amount, and porosity of the electrode. The mass loading amount of the cathode and anode, determined by the thickness and mixing ratio of the electroactive materials, directly influences the specific capacity, energy, power density, and overall performance of the LIBs. Thus, each step in the fabrication process should be carefully managed to meet the requirements of full-cell LIBs. The final cost of full-cell LIBs is influenced by the costs of materials, cell components, and manufacturing processes, necessitating the optimization of cost analysis for each component to minimize the overall expense.

Consequently, numerous parameters have been specifically designed, modified, and optimized to enhance the efficiency of full-cell LIBs. Critical parameters include the form factor (shapes and dimensions) of the battery, choice of materials for the main component, and factors affecting performance such as the electrochemical potential window, electrochemical reaction chemistry, conductivity, efficiency, and thermodynamics. The last factor to be considered is productivity and cost of LIBs. It is essential to apply standard synthesis techniques with meticulous care, including structural and surface treatments to enhance intrinsic and extrinsic properties, as well as to employ novel *in situ* and *ex situ* technological approaches to assess the precise performance of full-cell LIBs under extreme temperatures. Additionally, understanding the physicochemical factors that influence LIB performance and preventing impurities that could cause internal short circuits are crucial. Therefore, a thorough investigation of electrode fabrication and cell assembly processes is necessary to achieve high-energy density and high-performance full-cell LIBs.

**Author Contributions:** Conceptualization, methodology, and software, F.G. and D.L.; writing—original draft preparation, F.G.; writing—review and editing, D.L. and K.A.; visualization, supervision, project administration, and funding acquisition, D.L. All authors have read and agreed to the published version of the manuscript.

**Funding:** This work was supported by the National R&D Program from Ministry of Trade, Industry and Energy of Korea (20021922).

**Data Availability Statement:** Not applicable.

**Conflicts of Interest:** The authors declare no conflicts of interest.

## References

1. Behabtu, H.A.; Messagie, M.; Coosemans, T.; Berecibar, M.; Fante, K.A.; Kebede, A.A.; Mierlo, J.V. A review of energy storage technologies: Application potentials in renewable energy sources grid integration. *Sustainability* **2020**, *12*, 10511. [[CrossRef](#)]
2. China Energy Storage Alliance (CNESA). CNESA Global Energy Storage Market Analysis-2019; Q4 (Summary); China Energy Storage Alliance (CNESA): Beijing, China, 2020.
3. Whittingham, M.S. Electrical energy storage and intercalation chemistry. *Science* **1976**, *192*, 1126–1127. [[CrossRef](#)]
4. Whittingham, M.S.; Jacobson, A.J. *Intercalation Chemistry*; Academic Press: New York, NY, USA, 1982.
5. Nagaura, T.; Nagamine, M.; Tanabe, I.; Miyamoto, N. Solid-state batteries with sulfide-based electrolytes. *Prog. Batter. Sol. Cells* **1989**, *8*, 84–88.
6. Yazami, R.; Touzain, P. A reversible graphit-lithium negative electrode for electrochemical generators. *J. Power Sources* **1983**, *9*, 365–371. [[CrossRef](#)]
7. Sarre, G.; Blanchard, P.; Broussely, M. Aging of lithium-ion batteries. *J. Power Sources* **2004**, *127*, 65–71. [[CrossRef](#)]
8. Guo, J.; Li, Y.; Pedersen, K.; Stroe, D.-I. Lithium-ion battery, operation, degradation, and aging mechanism in electric vehicles: An overview. *Energies* **2021**, *14*, 5220. [[CrossRef](#)]
9. Zhang, X.; Li, P.; Huang, B.; Zhang, H. Numerical investigation on the thermal behavior of cylindrical lithium-ion batteries based on the electrochemical thermal coupling model. *Int. J. Heat Mass Transf.* **2022**, *199*, 123449. [[CrossRef](#)]
10. Román-Ramírez, L.; Marco, J. Design of Experiments Applied to Lithium-Ion Batteries: A Literature Review. *Appl. Energy* **2022**, *320*, 119305. [[CrossRef](#)]

11. Kim, H.-J.; Krishna, T.N.V.; Zeb, K.; Rajangam, V.; Gopi, C.V.V.M.; Sambasivam, S.; Raghavendra, K.V.G.; Obaidat, I.M. A comprehensive review of Li-ion battery materials and Their recycling techniques. *Electronics* **2020**, *9*, 1161. [[CrossRef](#)]
12. Barbosa, J.C.; Goncalves, R.; Costa, C.M.; Mendez, S.L. Recent advances on Materials for Lithium-ion batteries. *Energies* **2021**, *14*, 3145. [[CrossRef](#)]
13. Kim, T.; Song, W.; Son, D.-Y.; Ono, L.K.; Qi, Y. Lithium-ion batteries: Outlook on present, future, and hybridized technologies. *J. Mater. Chem. A* **2019**, *7*, 2942–2964. [[CrossRef](#)]
14. Chaudhary, M.; Tyagi, S.; Gupta, R.K.; Singh, B.P.; Singhal, R. Surface modification of cathode materials for energy storage devices: A review. *Surf. Coat. Technol.* **2021**, *412*, 127009. [[CrossRef](#)]
15. Wang, Y.; Xiao, X.; Li, Q.; Pang, H. Synthesis and Progress of New Oxygen vacant electrode materials for high-energy rechargeable battery applications. *Small* **2018**, *14*, 1802193. [[CrossRef](#)] [[PubMed](#)]
16. Ji, X.; Xia, Q.; Xu, Y.; Feng, H.; Wang, P.; Tan, Q. A review on progress of lithium-rich manganese-based cathodes for lithium-ion batteries. *J. Power Sources* **2021**, *487*, 229362. [[CrossRef](#)]
17. Fayaz, H.; Afzal, A.; Samee, A.D.M.; Soudagar, M.E.M.; Akram, N.; Mujtaba, M.A.; Jilte, M.; Islam, T.; Agbulut, U.; Saleel, C.A. Optimization of Thermal and Structural Design in Lithium-Ion Batteries to Obtain Energy Efficient Battery Thermal Management System (BTMS): A Critical Review. *Arch. Comput. Methods Eng.* **2022**, *29*, 129–194. [[CrossRef](#)]
18. Du, S.; Lai, Y.; Ai, L.; Ai, L.; Cheng, Y.; Tang, Y.; Jia, M. An investigation of irreversible heat generation in lithium-ion batteries based on a thermo-electrochemical coupling method. *Appl. Therm. Eng.* **2017**, *121*, 501–510. [[CrossRef](#)]
19. Goriparti, S.; Miele, E.; De Angelis, F.; Di Fabrizio, E.; Zaccaria, R.P.; Capiglia, C. Review on recent progress of nanostructured anode materials for Li-ion batteries. *J. Power Sources* **2014**, *257*, 421–443. [[CrossRef](#)]
20. Li, J.; Zhong, W.; Deng, Q.; Zhang, Q.; Yang, C. Recent progress in synthesis and surface modification of Nickle-rich layered oxide cathode materials for lithium-ion batteries. *Int. J. Extrem. Manuf.* **2022**, *4*, 042004. [[CrossRef](#)]
21. Zhang, J.; Qiao, J.; Sun, K.; Wang, Z. Balancing particle properties for practical lithium-ion batteries. *Particuology* **2022**, *61*, 18–29. [[CrossRef](#)]
22. Mayur, M.; DeCaluwe, S.C.; Kee, B.L.; Bessler, W.G. Modeling and simulation of the thermodynamics of lithium-ion battery intercalation materials in the open-source software Cantera. *Electrochim. Acta* **2019**, *323*, 134797. [[CrossRef](#)]
23. Kim, J.-S.; Lee, D.-C.; Lee, J.-J.; Kim, C.-W. Optimization for the maximum specific energy density of a lithium-ion battery using progressive quadratic response surface method and design of experiments. *Sci. Rep.* **2020**, *10*, 15586. [[CrossRef](#)] [[PubMed](#)]
24. Lain, M.J.; Brandon, J.; Kendrick, E. Design Strategies for High Power vs. High Energy Lithium-Ion Cells. *Batteries* **2019**, *5*, 64. [[CrossRef](#)]
25. Tikekar, M.D.; Choudhury, S.; Tu, Z.; Archer, L.A. Design principles for electrolytes and interfaces for stable lithium-metal batteries. *Nat. Energy* **2016**, *1*, 16114. [[CrossRef](#)]
26. Park, S.; Jeong, S.Y.; Lee, T.K.; Park, M.W.; Lim, H.Y.; Sung, J.; Cho, J.; Kwak, S.K.; Hong, S.Y.; Choi, N.-S. Replacing conventional battery electrolyte additives with dioxolone derivatives for high-energy-density lithium-ion batteries. *Nat. Commun.* **2021**, *12*, 838. [[CrossRef](#)] [[PubMed](#)]
27. Khan, F.N.U.; Rasul, M.G.; Sayem, A.S.M.; Mandal, N.K. Design and optimization of lithium-ion battery as an efficient energy storage device for electric vehicles: A comprehensive review. *J. Energy Storage* **2023**, *71*, 108033. [[CrossRef](#)]
28. XU, J.; Cai, X.; Cai, S.; Shao, Y.; Hu, C.; Lu, S.; Ding, S. High-energy lithium-ion batteries: Recent progress and a promising future in applications. *Energy Environ. Mater.* **2023**, *6*, e12450. [[CrossRef](#)]
29. Wang, Q.; O'Carroll, T.; Shi, F.; Huang, Y.; Chen, G.; Yang, X.; Nevar, A.; Dudko, N.; Tarasenko, N.; Xie, J.; et al. Designing Organic Material Electrodes for Lithium-Ion Batteries: Progress, Challenges, and Perspectives. *Electrochem. Energy Rev.* **2024**, *7*, 15. [[CrossRef](#)]
30. Chawla, N.; Bharti, N.; Singh, S. Recent Advances in Non-flammable electrolytes for safer lithium-ion batteries. *Batteries* **2019**, *5*, 19. [[CrossRef](#)]
31. Zhu, L.; Bao, C.; Xie, L.; Yang, X.; Cao, X. Review of synthesis and structural optimization of LiNi<sub>1/3</sub>Co<sub>1/3</sub>Mn<sub>1/3</sub>O<sub>2</sub> cathode materials for lithium-ion batteries applications. *J. Alloys Comp.* **2020**, *831*, 154864. [[CrossRef](#)]
32. Ren, D.; Shen, Y.; Yang, Y.; Shen, L.; Levin, B.D.A.; Yu, Y.; Muller, D.A.; Arbuna, H.D. Systematic optimization of battery materials: Key parameter optimization for the scalable synthesis of uniform high-energy, and high-stability LiNi<sub>0.6</sub>Mn<sub>0.2</sub>Co<sub>0.2</sub>O<sub>2</sub> cathode materials for Lithium-ion batteries. *ACS Appl. Mater. Interfaces* **2017**, *9*, 35811–35819. [[CrossRef](#)]
33. Julien, C.; Mauger, A.; Zaghib, K.; Groult, H. Optimization of layered cathode materials for Lithium-ion batteries. *Materials* **2016**, *9*, 595. [[CrossRef](#)] [[PubMed](#)]
34. Manthiram, A.; Chemelewski, K.; Lee, E.-S. A perspective on the high-voltage LiMn<sub>1.5</sub>Ni<sub>0.5</sub>O<sub>4</sub> spinel cathode for lithium-ion batteries. *Energy Environ. Sci.* **2014**, *7*, 1339–1350. [[CrossRef](#)]
35. Zheng, J.; Ye, Y.; Pan, F. Structure units as material genes in cathode materials for lithium-ion batteries. *Natl. Sci. Rev.* **2020**, *7*, 242–245. [[CrossRef](#)]
36. Zheng, J.; Xiao, J.; Zhang, J.-G. The roles of oxygen non-stoichiometry on the electrochemical properties of oxide-based cathode materials. *Nano Today* **2016**, *11*, 678–694. [[CrossRef](#)]
37. Kuganathan, N.; Ganeshalingham, S.; Chroneos, A. Defects, Dopants and Lithium mobility in Li<sub>9</sub>V<sub>3</sub>(P<sub>2</sub>O<sub>7</sub>)<sub>3</sub>(PO<sub>4</sub>)<sub>2</sub>. *Sci. Rep.* **2018**, *8*, 8140. [[CrossRef](#)]

38. Kuganathan, N.; Soloviov, A.L.; Vovk, R.V.; Chroneos, A. Defects, diffusion, and dopants in  $\text{Li}_8\text{SnO}_6$ . *Heliyon* **2021**, *7*, e07460. [[CrossRef](#)]
39. Zhang, J.; Jiang, H.; Zeng, Y.; Zhang, Y.; Guo, H. Oxygen-defective  $\text{Co}_3\text{O}_4$  for pseudo-capacitive lithium storage. *J. Power Sources* **2019**, *439*, 227026. [[CrossRef](#)]
40. Wang, F.; Wang, X.; Chang, Z.; Zhu, Y.; Fu, L.; Liu, X.; Wu, Y. Electrode materials with tailored facets for electrochemical energy storage. *Nanoscale Horiz.* **2016**, *1*, 272–289. [[CrossRef](#)]
41. Guo, B.; Ruan, H.; Zheng, C.; Fei, H.; Wei, M. Hierarchical  $\text{LiFePO}_4$  with a controllable growth of the (010) facet for lithium-ion batteries. *Sci. Rep.* **2013**, *3*, 2788. [[CrossRef](#)]
42. Zhang, F.; Lou, S.; Li, S.; Yu, Z.; Liu, Q.; Dai, A.; Cao, C.; Toney, M.F.; Ge, M.; Xiao, X.; et al. Surface regulation enables high stability of single-crystal lithium-ion cathodes at high voltage. *Nat. Comm.* **2020**, *11*, 3050. [[CrossRef](#)]
43. Wang, Y.; Wang, E.; Zhang, X.; Yu, H. High-Voltage Single-Crystal Cathode materials for Lithium-Ion Batteries. *Energy Fuels* **2021**, *35*, 1918–1932. [[CrossRef](#)]
44. Langdon, J.; Manthiram, A. A perspective on single-crystal layered oxide cathodes for lithium-ion batteries. *Energy Storage Mater.* **2021**, *37*, 143–160. [[CrossRef](#)]
45. Qian, G.; Zhang, Y.; Li, L.; Zhang, R.; Xu, J.; Cheng, Z.; Xie, S.; Wang, H.; Rao, Q.; He, Y.; et al. Single crystal Nickel-rich layered oxide battery cathode materials: Synthesis, electrochemistry, and intra-granular fracture. *Energy Storage Mater.* **2020**, *27*, 140–149. [[CrossRef](#)]
46. Lu, C.-H.; Lin, S.-W. Influence of the particle size on the electrochemical properties of lithium manganese oxide. *J. Power Sources* **2001**, *97–98*, 458–460. [[CrossRef](#)]
47. Majdabadi, M.M.; Farhad, S.; Farkhondeh, M.; Fraser, R.A.; Fowler, M. Simplified electrochemical multi-particle model for  $\text{LiFePO}_4$  cathodes in lithium-ion batteries. *J. Power Sources* **2015**, *275*, 633–643. [[CrossRef](#)]
48. Wu, S.; Yu, B.; Wu, Z.; Fang, S.; Shi, B.; Yang, J. Effect of particle size distribution on the electrochemical performance of micro-sized silicon-based negative materials. *RSC Adv.* **2018**, *8*, 8544–8551. [[CrossRef](#)]
49. Zhu, G.; Wang, Y.; Yang, S.; Qu, Q.; Zheng, H. Correlation between the physical parameters and the electrochemical performance of a silicon anode in lithium-ion batteries. *J. Mater.* **2019**, *5*, 164–175. [[CrossRef](#)]
50. Garcia, J.C.; Barenco, J.; Yan, J.; Chen, G.; Hauser, A.; Croy, J.R.; Iddir, H. Surface structure, morphology, and stability of  $\text{LiNi}_{1/3}\text{Mn}_{1/3}\text{Co}_{1/3}\text{O}_2$  cathode material. *J. Phys. Chem. C* **2017**, *121*, 8290–8299. [[CrossRef](#)]
51. Li, H.; Ren, Y.; Yang, P.; Jian, Z.; Wang, W.; Xing, Y.; Zhang, S. Morphology, and size-controlled synthesis of the hierarchical structured  $\text{Li}_{1.2}\text{Mn}_{0.54}\text{Ni}_{0.13}\text{Co}_{0.13}\text{O}_2$  cathode materials for lithium-ion batteries. *Electrochim. Acta* **2019**, *297*, 406–416. [[CrossRef](#)]
52. Wei, C.; He, W.; Zhang, X.; Xu, F.; Liu, Q.; Sun, C.; Song, X. Effect of morphology on the electrochemical performance  $\text{Li}_3\text{V}_2(\text{PO}_4)_3$  cathode materials for lithium-ion batteries. *RSC Adv.* **2015**, *5*, 54225–54245. [[CrossRef](#)]
53. Wang, S.; Zhang, Z.; Jiang, Z.; Deb, A.; Yang, L.; Hirano, S.-I. Mesoporous  $\text{Li}_3\text{V}_2(\text{PO}_4)_3@\text{CMK}-3$  nanocomposite cathode material for lithium-ion batteries. *J. Power Sources* **2014**, *253*, 294–299. [[CrossRef](#)]
54. Muller, M.; Schneider, L.; Bohn, N.; Binder, J.R.; Bauer, W. Effect of nanostructured and open-porous particle morphology on electrodes processing and electrochemical performance of Li-ion batteries. *ACS Appl. Energy Mater.* **2021**, *4*, 1993–2003. [[CrossRef](#)]
55. Seher, J.; Froba, M. Shape Matters: The effect of particle morphology on the fast-charging performance of  $\text{LiFePO}_4/\text{C}$  nanoparticle composite electrode. *ACS Omega* **2021**, *6*, 24062–24069. [[CrossRef](#)] [[PubMed](#)]
56. Ghani, F.; Raza, A.; Kyung, D.; Kim, H.-S.; Lim, J.C.; Nah, I.W. Optimization of synthesis conditions of high-tap density  $\text{FeVO}_4$  hollow microspheres via spray pyrolysis for lithium-ion batteries. *Appl. Surf. Sci.* **2019**, *497*, 143718. [[CrossRef](#)]
57. Birk, C.R.; Roberts, M.R.; McTurk, E.; Bruce, P.G.; Howey, D.A. Degradation diagnostics for lithium-ion cells. *J. Power Sources* **2017**, *341*, 373–386. [[CrossRef](#)]
58. Liu, H.; Wolfman, M.; Karki, K.; Yu, Y.-S.; Stach, E.A.; Cabana, J.; Chapman, K.W.; Chupas, P.J. Intergranular cracking as a major cause of long-term capacity fading of layered cathodes. *Nano Lett.* **2017**, *17*, 3452–3457. [[CrossRef](#)]
59. Lei, Y.; Ni, J.; Hu, Z.; Wang, Z.; Gui, F.; Li, B.; Ming, P.; Zhang, C.; Elias, Y.; Aurbach, D.; et al. Surface modification of Li-rich Mn-based layered oxide cathodes: Challenges, materials, methods, and characterization. *Adv. Energy Mater.* **2020**, *10*, 2002506. [[CrossRef](#)]
60. Raza, A.; Ghani, F.; Lim, J.C.; Nah, I.W.; Kim, H.-S. Eco-friendly prepared mesoporous carbon encapsulated  $\text{SnO}_2$  nanoparticles for high-reversible lithium-ion battery anodes. *Microporous Mesoporous Mater.* **2021**, *314*, 110853. [[CrossRef](#)]
61. Palacin, M.R. Recent Advances in rechargeable battery materials: A chemist's perspective. *Chem. Soc. Rev.* **2009**, *38*, 2565–2575. [[CrossRef](#)]
62. Cheng, H.; Shapter, J.G.; Li, Y.; Gao, G. Recent progress of advanced anode materials of lithium-ion batteries. *J. Energy Chem.* **2021**, *57*, 451–468. [[CrossRef](#)]
63. Bensalah, N.; Dawood, H. Review on synthesis, characterizations, and electrochemical properties of cathode materials for Lithium-ion batteries. *J. Mater. Sci. Eng.* **2016**, *5*, 4.
64. Lyu, Y.; Wu, X.; Wang, K.; Feng, Z.; Cheng, T.; Liu, Y.; Wang, M.; Chen, R.; Xu, L.; Zhou, J.; et al. An overview on the advances of  $\text{LiCoO}_2$  cathodes for Lithium-Ion Batteries. *Adv. Energy Mater.* **2021**, *11*, 2000982. [[CrossRef](#)]
65. Liu, L.; Li, M.; Chu, L.; Jiang, B.; Lin, R.; Zhu, X.; Cao, G. Layered ternary metal oxides: Performance degradation mechanisms as cathodes, and design strategies for high-performance batteries. *Prog. Mater. Sci.* **2020**, *111*, 100655. [[CrossRef](#)]

66. Kim, K.H.; Jeong, H.; Lee, H.C.; Shon, J.K.; Park, J.; Park, H.-Y. Stable cycling of high-density three-dimensional sintered LiCoO<sub>2</sub> plate cathodes. *J. Power Sources* **2022**, *551*, 232223. [[CrossRef](#)]
67. Lv, Y.; Huang, S.; Zhao, Y.; Roy, S.; Lu, X.; Hou, Y.; Zhang, J. A review of nickel-rich layered oxides cathodes: Synthetic strategies, structural characteristics, failure mechanism, improvement approaches and prospects. *Appl. Energy* **2022**, *305*, 117849. [[CrossRef](#)]
68. Aishova, A.; Park, G.-T.; Yoon, C.S.; Sun, Y.-K. Cobalt-free high-capacity Ni-rich layered Li [Ni<sub>0.9</sub>Mn<sub>0.1</sub>] O<sub>2</sub> cathode. *Adv. Energy Mater.* **2020**, *10*, 1903179. [[CrossRef](#)]
69. Zhang, Q.; Su, Y.; Chen, L.; Lu, Y.; Bao, L.; He, T. Pre-oxidizing the precursors of Nickel-rich cathode materials to regulate their Li<sup>+</sup>/Ni<sup>2+</sup> cation ordering towards cyclability improvements. *J. Power Sources* **2018**, *396*, 734–741. [[CrossRef](#)]
70. Sun, J.; Cao, X.; Zhou, H. Advanced single-crystal layered Ni-rich cathode materials for next-generation high-energy density and long-life Li-ion batteries. *Phys. Rev. Mater.* **2022**, *6*, 070201. [[CrossRef](#)]
71. Zuo, W.; Luo, M.; Liu, X.; Wu, J.; Liu, H.; Li, J.; Winter, M.; Fu, R.; Yang, W.; Yang, Y. Li-rich cathodes for rechargeable Li-based batteries: Reaction mechanisms and advanced characterization techniques. *Energy Environ. Sci.* **2020**, *13*, 4450–4497. [[CrossRef](#)]
72. Zheng, H.; Han, X.; Guo, W.; Lin, L.; Xie, Q.; Liu, P.; He, W.; Wang, L.; Peng, D.-L. Recent developments and challenges of Li-rich Mn-based cathode materials for high-energy lithium-ion batteries. *Mater. Today Energy* **2020**, *18*, 100518. [[CrossRef](#)]
73. Li, Q.; Ning, D.; Wong, D.; An, K.; Tang, Y.; Zhou, D.; Schuck, G.; Chen, Z.; Zhang, N.; Liu, X. Improving the oxygen redox reversibility of Li-rich battery cathode materials via coulombic repulsive interactions strategy. *Nat. Commun.* **2022**, *13*, 1123. [[CrossRef](#)] [[PubMed](#)]
74. Cui, C.; Fan, X.; Zhou, X.; Chen, J.; Wang, Q.; Ma, L.; Yang, C.; Hu, E.; Yang, X.-Q.; Wang, C. Structure and interface design enable stable Li-rich cathode. *J. Am. Chem. Soc.* **2020**, *142*, 8918–8927. [[CrossRef](#)] [[PubMed](#)]
75. Tan, H.T.; Rui, X.; Sun, W.; Yan, Q.; Lim, T.M. Vanadium-based nanostructure materials for secondary lithium battery applications. *Nanoscale* **2015**, *7*, 14595. [[CrossRef](#)] [[PubMed](#)]
76. Huang, X.; Rui, X.; Hng, H.H.; Yan, Q. Vanadium pentoxide-based cathode materials for Lithium-Ion Batteries: Morphology control, carbon hybridization, and cation doping. *Part. Part. Syst. Charact.* **2015**, *32*, 276–294. [[CrossRef](#)]
77. Chen, H.; Cheng, S.; Chen, D.; Jiang, Y.; Ang, E.H.; Liu, W.; Feng, Y.; Rui, X.; Yu, Y. Vanadate-based electrodes for rechargeable batteries. *Mater. Chem. Front.* **2021**, *5*, 1585. [[CrossRef](#)]
78. Radzi, Z.I.; Arifin, K.H.; Kufian, M.Z.; Balakrishnan, V.; Raihan, S.R.S.; Rahim, N.A.; Subramanian, R. Review of spinal LiMn<sub>2</sub>O<sub>4</sub> cathode materials under high cut-off voltage in lithium-ion batteries: Challenges and strategies. *J. Electroanal. Chem.* **2022**, *920*, 116623. [[CrossRef](#)]
79. Ma, J.; Hu, P.; Cui, G.; Chen, L. Surface and Interface Issues in spinel LiNi<sub>0.5</sub>Mn<sub>1.5</sub>O<sub>4</sub>: Insights into a potential cathode material for High-energy density lithium-ion batteries. *Chem. Mater.* **2016**, *28*, 3578–3606. [[CrossRef](#)]
80. Xu, X.; Deng, S.; Wang, H.; Liu, J.; Yan, H. Research progress in improving the cycling stability of high-voltage LiNi<sub>0.5</sub>Mn<sub>1.5</sub>O<sub>4</sub> cathode in Lithium-Ion Battery. *Nano-Micro Lett.* **2017**, *9*, 22. [[CrossRef](#)]
81. Ling, J.; Karuppiyah, C.; Krishnan, S.G.; Reddy, M.V.; Misnon, I.I.; Rahim, M.H.A.; Yang, C.-C.; Jose, R. Phosphate polyanion materials as high-voltage lithium-ion battery cathodes: A Review. *Energy Fuels* **2021**, *35*, 10428–10450. [[CrossRef](#)]
82. Peng, Y.; Tan, R.; Ma, J.; Li, Q.; Wang, T.; Duan, X. Electrospun Li<sub>3</sub>V<sub>2</sub>(PO<sub>4</sub>)<sub>3</sub> nanocubes/carbon nanofibers as free-standing cathodes for high-performance lithium-ion batteries. *J. Mater. Chem. A* **2019**, *7*, 14681–14688. [[CrossRef](#)]
83. Hu, J.; Huang, W.; Yang, L.; Pan, F. Structure and performance of the LiFePO<sub>4</sub> cathode material: From the bulk to the surface. *Nanoscale* **2020**, *12*, 15036–15044. [[CrossRef](#)] [[PubMed](#)]
84. Ramsubramanian, B.; Sundarrajan, S.; Chellappan, V.; Reddy, M.V.; Ramakrishna, S.; Zaghib, K. Recent development in carbon-LiFePO<sub>4</sub> cathode for Lithium-Ion Batteries: A Mini-Review. *Batteries* **2022**, *8*, 133. [[CrossRef](#)]
85. Islam, M.S.; Dominko, R.; Masquelier, C.; Sirisopanaporn, C.; Armstrong, A.R.; Bruce, P.G. Silicate cathodes for lithium batteries: Alternatives to phosphates? *J. Mater. Chem.* **2011**, *21*, 9811–9818. [[CrossRef](#)]
86. Bao, L.; Gao, W.; Su, Y.; Wang, Z.; Li, N.; Chen, S.; Wu, F. Progression of the silicate cathode materials used in lithium-ion batteries. *Chin. Sci. Bull.* **2013**, *58*, 575–584. [[CrossRef](#)]
87. Yang, S.-H.; Xue, H.; Guo, S.-P. Borates as promising electrode materials for rechargeable batteries. *Coord. Chem. Rev.* **2021**, *427*, 213551. [[CrossRef](#)]
88. Ma, T.; Muslim, A.; Su, Z. Microwave synthesis and electrochemical properties of lithium manganese borate as cathode for lithium-ion batteries. *J. Power Sources* **2015**, *282*, 95–99. [[CrossRef](#)]
89. Daniel, C.; Mohanty, D.; Li, J.; Wood, D.L. Review on Electrochemical Storage Materials and Technology. *AIP Conf. Proc.* **2014**, *1597*, 26–43.
90. Ghosh, S.; Bhattacharjee, U.; Bhowmik, S.; Martha, S.K. A Review on High-Capacity and High-Voltage Cathodes for Next-Generation Lithium-ion Batteries. *J. Energy Power Technol.* **2022**, *1*, 2. [[CrossRef](#)]
91. Asenbauer, J.; Eisenmann, T.; Kuenzel, M.; Kazzazi, A.; Chen, Z.; Bresser, D. The success story of graphite as a lithium-ion anode material—fundamentals, remaining challenges, and recent developments including silicon (oxide) composites. *Sustain. Energy Fuels* **2020**, *4*, 5387. [[CrossRef](#)]
92. Chang, H.; Wu, Y.-R.; Han, X.; Yi, T.-F. Recent developments in advanced anode materials for lithium-ion batteries. *Energy Mater.* **2021**, *1*, 100003. [[CrossRef](#)]
93. Zhao, W.; Choi, W.; Yoon, W.-S. Nanostructured Electrode materials for rechargeable Lithium-Ion batteries. *J. Electrochem. Sci. Technol.* **2020**, *11*, 195–219. [[CrossRef](#)]

94. Ma, D.; Cao, Z.; Hu, A. Si-based Anode materials for Li-ion batteries: A mini review. *Nano-Micro Lett.* **2014**, *6*, 347–358. [CrossRef] [PubMed]
95. Fang, S.; Bresser, D.; Passerini, S. Transition metal oxide anodes for electrochemical energy storage in Lithium- and Sodium-Ion Batteries. *Adv. Energy Mater.* **2020**, *10*, 1902485. [CrossRef]
96. Nzereogu, P.U.; Omah, A.D.; Ezema, F.I.; Iwuoha, E.I.; Nwanya, A.C. Anode materials for lithium-ion batteries: A review. *Appl. Surf. Sci. Adv.* **2022**, *9*, 100233. [CrossRef]
97. Parikh, P.; Sina, M.; Banerjee, A.; Wang, X.; D’Souza, M.S.; Doux, J.-M.; Wu, E.A.; Trieu, O.Y.; Gong, Y.; Zhou, Q.; et al. Role of polyacrylic acid (PAA) Binder on the solid electrolyte interphase in silicon anodes. *Chem. Mater.* **2019**, *31*, 2535–2544. [CrossRef]
98. Jiang, S.; Hu, B.; Shi, Z.; Chen, W.; Zhang, Z.; Zhang, L. Re-Engineering Poly (Acrylic Acid) Binder toward optimized electrochemical performance for silicon lithium-ion batteries: Branching Architecture leads to balanced properties of polymeric binders. *Adv. Funct. Mater.* **2020**, *30*, 1908558. [CrossRef]
99. Chen, J.; Liu, J.; Qi, Y.; Sun, T.; Li, X. Unveiling the roles of binder in the mechanical integrity of electrodes for Lithium-ion batteries. *J. Electrochem. Soc.* **2013**, *160*, A1502–A1509. [CrossRef]
100. Dong, T.; Mu, P.; Zhang, S.; Zhang, H.; Liu, W.; Cui, G. How Do Polymer Binders Assist Transition Metal Oxide Cathodes to Address the Challenge of High-Voltage Lithium Battery Applications? *Electrochem. Energy Rev.* **2021**, *4*, 545–565. [CrossRef]
101. Shi, Y.; Zhou, X.; Yu, G. Material and Structural Design of Novel Binder Systems for High-Energy, High-power Lithium-ion batteries. *Acc. Chem. Res.* **2017**, *50*, 2642–2652. [CrossRef]
102. Kazzazi, A.; Bresser, D.; Birrozzzi, A.; van Zamory, J.; Hekmatfar, M.; Passerini, S. Comparative analysis of aqueous binders for high-energy Li-rich NMC as a lithium-ion cathode and the impact of adding phosphoric acid. *ACS Appl. Mater. Interfaces* **2018**, *10*, 17214–17222. [CrossRef]
103. He, J.; Wei, Y.; Hu, L.; Li, H.; Zhai, T. Aqueous binders enhanced high-performance GeP<sub>5</sub> anode for lithium-ion batteries. *Front. Chem.* **2018**, *6*, 21. [CrossRef] [PubMed]
104. Bresser, D.; Buchholz, D.; Moretti, A.; Varzi, A.; Passerini, S. Alternative binders for sustainable electrochemical energy storage—the transition to aqueous electrode processing and bio-derived polymers. *Energy Environ. Sci.* **2018**, *11*, 3096–3127. [CrossRef]
105. Fitz, O.; Ingenhoven, S.; Bischoff, C.; Gentischer, H.; Birke, K.P.; Saracsan, D.; Biro, D. Comparison of aqueous and non-aqueous based binder polymers and the mixing ratio of Zn//MnO<sub>2</sub> batteries with mildly acidic aqueous electrolytes. *Batteries* **2021**, *7*, 40. [CrossRef]
106. Wang, R.; Feng, L.; Yang, W.; Zhang, Y.; Zhang, Y.; Bai, W.; Liu, B.; Zhang, W.; Chuan, Y.; Zheng, Z.; et al. Effect of different binders on the electrochemical performance of metal oxide anode for lithium-ion batteries. *Nanoscale Res. Lett.* **2017**, *12*, 575. [CrossRef]
107. Xing, J.; Bliznakov, S.; Bonville, L.; Oljace, M.; Maric, R. A review of non-aqueous electrolytes, binders, and separators for lithium-ion batteries. *Electrochem. Energy Rev.* **2022**, *5*, 14. [CrossRef]
108. Cholewinski, A.; Si, P.; Uceda, M.; Pope, M.; Zhao, B. Polymer Binders: Characterization and development towards aqueous electrode fabrication for sustainability. *Polymers* **2021**, *13*, 631. [CrossRef]
109. Yim, T.; Choi, S.J.; Jo, Y.N.; Kim, T.-H.; Kim, K.J.; Jeong, G.; Kim, Y.-J. Effect of binder properties on electrochemical performance for silicon-graphite anode: Method and application of binder screening. *Electrochim. Acta* **2014**, *136*, 112–120. [CrossRef]
110. Rapisarda, M.; Marken, F.; Meo, M. Graphene oxide and starch gel as a hybrid binder for environmentally friendly high-performance supercapacitors. *Commun. Chem.* **2021**, *4*, 169. [CrossRef] [PubMed]
111. Kannan, D.R.R.; Terala, P.K.; Moss, P.L.; Weatherspoon, M.H. Analysis of the separator thickness and porosity on the performance of lithium-ion batteries. *Intl. J. Electrochem.* **2018**, *2018*, 1925708.
112. Kim, P.J. Surface-functionalized separator for stable and reliable lithium-ion batteries: A review. *Nanomaterials* **2021**, *11*, 2275. [CrossRef]
113. Yuan, M.; Liu, K. Rational design on separators and liquid electrolytes for safer lithium-ion batteries. *J. Energy Chem.* **2020**, *43*, 58–70. [CrossRef]
114. Chen, K.; Li, Y.; Zhan, H. Advanced separators for lithium-ion batteries. *Earth Environ. Sci.* **2022**, *1011*, 012009. [CrossRef]
115. Ding, L.; Yan, N.; Zhang, S.; Xu, R.; Wu, T.; Wang, F.; Cao, Y.; Xiang, M. Facile manufacture technique for lithium-ion batteries composite separator via online construction of fumed SiO<sub>2</sub> coating. *Mater. Des.* **2022**, *215*, 110476. [CrossRef]
116. Kim, G.; Noh, J.H.; Lee, H.; Shin, J.; Lee, D. Roll-to-Roll Gravure Coating of PVDF on a Battery Separator for the Enhancement of Thermal Stability. *Polymers* **2023**, *15*, 4108. [CrossRef] [PubMed]
117. Liu, Z.; Jiang, Y.; Hu, Q.; Guo, S.; Yu, L.; Li, Q.; Liu, Q.; Hu, X. Safer lithium-ion batteries from separator aspect: Development and future perspective. *Energy Environ. Mater.* **2021**, *4*, 336–362. [CrossRef]
118. Huang, X.; He, R.; Li, M.; Chee, M.O.L.; Dong, P.; Lu, J. Functionalized separator for next generation batteries. *Mat. Today* **2020**, *41*, 143–155. [CrossRef]
119. Lagadec, M.F.; Zahn, R.; Wood, V. Designing Polyolefin separators to minimize the impact of local compressive stresses on lithium-ion battery performance. *J. Electrochem. Soc.* **2018**, *165*, A1829–A1836. [CrossRef]
120. Zhu, P.; Gastol, D.; Marshall, J.; Sommerville, R.; Goodship, V.; Kendrick, E. A review of current collectors for lithium-ion batteries. *J. Power Sources* **2021**, *485*, 229321. [CrossRef]
121. Yamada, M.; Watanbe, T.; Gunji, T.; Wu, J.; Matsumoto, F. Review of the design of current collectors for improving the battery performance in lithium-ion and post lithium-ion batteries. *Electrochem* **2020**, *1*, 124–159. [CrossRef]

122. Harper, G.; Sommerville, R.; Kendrick, E.; Driscoll, L.; Slater, P.; Stolkin, R.; Walton, A.; Christensen, P.; Heidrich, O.; Lambert, S. Recycling lithium-ion batteries from electric vehicles. *Nature* **2019**, *575*, 75–86. [[CrossRef](#)]
123. Zhang, S.; Jow, T. Aluminum corrosion in electrolyte of Li-ion battery. *J. Power Sources* **2002**, *109*, 458–464. [[CrossRef](#)]
124. Kumar, P.S.; Ayyasamy, S.; Tok, E.S.; Adams, S.; Reddy, M. Impact of electrical conductivity on the electrochemical performance of layered structured Lithium Trivanadate ( $\text{LiV}_{3-x}\text{M}_x\text{O}_8$ ,  $\text{M} = \text{Zn}/\text{Co}/\text{Fe}/\text{Sn}/\text{Ti}/\text{Zr}/\text{Nb}/\text{Mo}$ ,  $x = 0.01\text{--}0.1$ ) as cathode material for energy storage. *ACS Omega* **2018**, *3*, 3036–3044. [[CrossRef](#)] [[PubMed](#)]
125. Nakamura, T.; Okano, S.; Yaguma, N.; Morinaga, Y.; Takahara, H.; Yamada, Y. Electrochemical performance of cathodes prepared on current collector with different surface morphologies. *J. Power Sources* **2013**, *244*, 532–537. [[CrossRef](#)]
126. Doberdo, I.; Loffler, N.; Laszczynski, N.; Cericola, D.; Penazzi, N.; Bodoardo, S.; Kim, G.-T.; Passerini, S. Enabling aqueous binder for lithium battery cathodes-carbon coating of aluminum current collector. *J. Power Sources* **2014**, *248*, 1000–1006. [[CrossRef](#)]
127. Boz, B.; Dev, T.; Salvadori, A.; Schaefer, J.L. Review-Electrolyte and Electrode Designs for enhanced ion transport properties to enable high performance lithium batteries. *J. Electrochem. Soc.* **2021**, *168*, 090501. [[CrossRef](#)]
128. Meutzner, F.; de Vivanco, M.U. Electrolytes-Technology review. *AIP Conf. Proc.* **2014**, *1597*, 185–195.
129. Chagnes, A.; Swiatowska, J. *Lithium Process Chemistry: Resources, Extractions, Batteries and Recycling*, 1st ed.; Elsevier: Amsterdam, The Netherland, 2015; Volume 5, pp. 167–189.
130. Zhang, H.; Liu, X.; Li, H.; Hasa, I.; Passerini, S. Challenges and Strategies for high-energy Aqueous Electrolytes rechargeable batteries. *Angew. Chem. Int. Ed.* **2021**, *60*, 598–616. [[CrossRef](#)]
131. Luo, J.-Y.; Cui, W.-J.; He, P.; Xia, Y.-Y. Raising the cycling stability of aqueous lithium-ion batteries by eliminating oxygen in the electrolyte. *Nat. Chem.* **2010**, *2*, 760–765. [[CrossRef](#)]
132. He, P.; Zhang, X.; Wang, Y.-G.; Cheng, L.; Xia, Y.-Y. Lithium-ion intercalation behavior of  $\text{LiFePO}_4$  in aqueous and nonaqueous electrolyte solutions. *J. Electrochem. Soc.* **2007**, *155*, A144. [[CrossRef](#)]
133. Xu, K. Nonaqueous liquid electrolytes for lithium-based rechargeable batteries. *Chem. Rev.* **2004**, *104*, 4303–4418. [[CrossRef](#)]
134. Zhang, S.; Li, J.; Jiang, N.; Li, X.; Pasupathi, S.; Fang, Y.; Liu, Q.; Dang, D. Rational Design of an Ionic Liquid-based electrolyte with High ionic conductivity towards safe Lithium/Lithium-Ion batteries. *Chem. Asian J.* **2019**, *14*, 2810–2814. [[CrossRef](#)] [[PubMed](#)]
135. Armand, M.; Endres, F.; MacFarlane, D.R.; Ohno, H.; Scrosati, B. Ionic-Liquid materials for the electrochemical challenges of the future. *Nat. Mater.* **2009**, *8*, 621–629. [[CrossRef](#)] [[PubMed](#)]
136. Lei, Z.; Chen, B.; Koo, Y.-M.; MacFarlane, D.R. Introduction: Ionic Liquids. *Chem. Rev.* **2017**, *117*, 6633–6635. [[CrossRef](#)] [[PubMed](#)]
137. Yu, Q.; Jiang, K.; Yu, G.; Chen, X.; Zhang, C.; Yao, Y.; Jiang, B.; Long, H. Recent progress of composite solid polymer electrolytes for all solid-state lithium metal batteries. *Chin. Chem. Lett.* **2021**, *32*, 2659–2678. [[CrossRef](#)]
138. Sasikumar, M.; Krishna, R.H.; Raja, M.; Therese, H.A.; Balakrishna, N.T.M.; Raghavan, P.; Sivakumar, P. Titanium dioxide nano-ceramic filler in solid polymer electrolytes: Strategy towards suppressed dendrite formation and enhanced electrochemical performance for safe lithium-ion batteries. *J. Alloys Compd.* **2021**, *882*, 160709. [[CrossRef](#)]
139. Suo, L.; Borodin, O.; Gao, T.; Olguin, M.; Ho, J.; Fan, X.; Luo, C.; Wang, C.; Xu, K. Water in salt electrolyte enables high-voltage aqueous lithium-ion chemistries. *Science* **2015**, *350*, 938–943. [[CrossRef](#)]
140. Chen, S.; Zhang, M.; Zou, P.; Sun, B.; Tao, S. Historical development, and novel concepts on electrolytes for aqueous rechargeable batteries. *Energy Environ. Sci.* **2022**, *15*, 1805–1839. [[CrossRef](#)]
141. Suo, L.; Oh, D.; Lin, Y.; Zhuo, Z.; Borodin, O.; Gao, T.; Wang, F.; Kushima, A.; Wang, Z.; Kim, H.-C.; et al. How solid-electrolyte interphase forms in aqueous electrolytes. *J. Am. Chem. Soc.* **2017**, *139*, 18670–18680. [[CrossRef](#)]
142. Yue, F.; Tie, Z.; Deng, S.; Wang, S.; Yang, M.; Niu, Z. An Ultralow Temperature Aqueous Battery with Proton Chemistry. *Angew. Chem. Int. Ed.* **2021**, *60*, 13882–13886. [[CrossRef](#)]
143. Sun, T.; Du, H.; Zheng, S.; Shi, J.; Tao, Z. High Power and Energy Density Aqueous Proton Battery Operated at  $-90^\circ\text{C}$ . *Adv. Funct. Mater.* **2021**, *31*, 2010127. [[CrossRef](#)]
144. Wang, F.; Borodin, O.; Ding, M.S.; Gobet, M.; Vatamanu, J.; Fan, X.; Gao, T.; Eidson, N.; Liang, Y.; Sun, W.; et al. Aqueous/Non-aqueous electrolyte for safe and high-energy Li-Ion batteries. *Joule* **2018**, *2*, 927–937. [[CrossRef](#)]
145. Chagnes, A.; Swiatowska, J. *New Developments in Lithium-Ion Batteries*, 1st ed.; Belharouak, I., Ed.; InTech: Vienna, Austria, 2012; Volume 6, pp. 145–172.
146. Hu, L.; Zhang, Z.; Amine, K. Electrochemical investigation of carbonate-based electrolytes for high voltage lithium-ion cells. *J. Power Sources* **2013**, *236*, 175–180. [[CrossRef](#)]
147. Yang, L.; Ravdel, B.; Lucht, B.L. Electrolyte Reaction with the surface of high voltage  $\text{LiNi}_{0.5}\text{Mn}_{1.5}\text{O}_4$  cathodes for Lithium-ion batteries. *Electrochim. Solid State Lett.* **2010**, *13*, A95–A97. [[CrossRef](#)]
148. Flamme, B.; Garcia, G.R.; Weil, M.; Haddad, M.; Phansavath, P.; Vidal, V.R.; Chagnes, A. Guidelines to design organic electrolytes for lithium-ion batteries: Environmental impact, physicochemical and electrochemical properties. *Green Chem.* **2017**, *19*, 1828–1849. [[CrossRef](#)]
149. Abe, K.; Ushigoe, Y.; Yoshitake, H.; Yoshio, M. Functional electrolytes: Novel type additives for cathode materials, providing high cycleability performance. *J. Power Sources* **2006**, *153*, 328–335. [[CrossRef](#)]
150. Assary, R.S.; Curtiss, L.A.; Redfern, P.C.; Zhang, Z.; Amine, K. Computational Studies of Polysiloxanes: Oxidation Potentials and Decomposition Reactions. *J. Phys. Chem. C* **2011**, *115*, 12216–12223. [[CrossRef](#)]
151. Nanbu, N.; Suzuki, Y.; Ohtsuki, K.; Meguro, T.; Takehara, M.; Ue, M.; Sasaki, Y. Physical and Electrochemical Properties of Monofluorinated Ethyl Acetates for Lithium Rechargeable Batteries. *Electrochemistry* **2010**, *78*, 446–449. [[CrossRef](#)]

152. McElroy, P.J.; Gellen, A.T.; Kolahi, S.S. Excess second virial coefficients and critical temperatures of methyl acetate and diethyl sulfide. *J. Chem. Eng. Data* **1990**, *35*, 38. [[CrossRef](#)]
153. Laurence, C.; Nicolet, P.; Dalati, M.T.; Abboud, J.-L.M.; Notario, R. The empirical treatment of solvent-solute interactions: 15 years of  $\pi^*$ . *J. Phys. Chem.* **1994**, *98*, 5807–5816. [[CrossRef](#)]
154. Obama, M.; Oodera, Y.; Kohama, N.; Yanase, T.; Saito, Y.; Kusano, K. Densities, molar volumes, and cubic expansion coefficients of 78 aliphatic ethers. *J. Chem. Eng. Data* **1985**, *30*, 1–5. [[CrossRef](#)]
155. Dutt, H.D.P.H.; Jeewan, R. Dielectric relaxation studies of oligether of ethylene glycol at microwave frequencies. *Bull. Chem. Soc. Jpn.* **1991**, *64*, 2030–2031.
156. Tobishima, S.-I.; Okada, T. Lithium cycling efficiency and conductivity for high dielectric solvent/low viscosity solvent mixed systems. *Electrochim. Acta* **1985**, *30*, 17151722. [[CrossRef](#)]
157. Mozhzhukhina, N.; Méndez De Leo, L.P.; Calvo, E.J. Infrared spectroscopy studies on stability of dimethyl sulfoxide for application in a Li-Air Battery. *J. Phys. Chem. C* **2013**, *117*, 18375–18380. [[CrossRef](#)]
158. Bennion, D.N.; Tiedemann, W.H. Density, viscosity, and conductivity of lithium trifluoromethanesulfonate solutions in dimethylsulfite. *J. Chem. Eng. Data* **1971**, *16*, 368. [[CrossRef](#)]
159. Svirbely, W.J.; Lander, J.J. The dipole moments of diethyl sulfite, triethyl phosphate and tetraethyl silicate. *J. Am. Chem. Soc.* **1948**, *70*, 4121. [[CrossRef](#)] [[PubMed](#)]
160. Chen, J.; Vatamanu, J.; Xing, L.; Borodin, O.; Chen, H.; Guan, X.; Liu, X.; Xu, K.; Li, W. Improving electrochemical stability and low-temperature performance with water/acetonitrile hybrid electrolyte. *Adv. Energy Mater.* **2020**, *10*, 1902654. [[CrossRef](#)]
161. Li, Q.; Chen, J.; Fan, L.; Kong, X.; Lu, Y. Progress in electrolytes for rechargeable Li-based batteries and beyond. *Green Energy Environ.* **2016**, *1*, 18–42. [[CrossRef](#)]
162. Pan, S.; Yao, M.; Zhang, J.; Li, B.; Xing, C.; Song, X.; Su, P.; Zhang, H. Recognition of ionic liquids as high-voltage electrolytes for supercapacitors. *Front. Chem.* **2020**, *8*, 261. [[CrossRef](#)]
163. Ahmad, S. Polymer Electrolyte: Characteristics and peculiarities. *Ionics* **2009**, *15*, 309–321. [[CrossRef](#)]
164. Xi, G.; Xiao, M.; Wang, S.; Han, D.; Li, Y.; Meng, Y. Polymer-based Solid Electrolytes: Material Selection, design, and Application. *Adv. Funct. Mater.* **2021**, *31*, 2007598. [[CrossRef](#)]
165. Zhao, Y.; Wang, L.; Zhou, Y.; Liang, Z.; Tavajohi, N.; Li, B.; Li, T. Solid Polymer Electrolytes with High Conductivity, and transference number of Li ions for Li-based rechargeable Batteries. *Adv. Sci.* **2021**, *8*, 2003675. [[CrossRef](#)] [[PubMed](#)]
166. Mackanic, D.G.; Yan, X.; Zhang, Q.; Matsuhisa, N.; Yu, Z.; Jiang, Y.; Manika, T.; Lopez, J.; Yan, H.; Chen, X.; et al. Decoupling of mechanical properties and ionic conductivity in supramolecular lithium-ion conductors. *Nat. Commun.* **2019**, *10*, 5384. [[CrossRef](#)]
167. An, Y.; Han, X.; Liu, Y.; Azhar, A.; Na, J.; Nanjundan, A.K.; Wang, S.; Yu, J.; Yamauchi, Y. Progress in Solid polymer electrolytes for lithium-ion batteries and beyond. *Small* **2022**, *18*, 2103617. [[CrossRef](#)]
168. Aravindan, V.; Gnanaraj, J.; Madhavi, S.; Liu, H.-K. Lithium-ion conducting electrolyte salts for lithium batteries. *Chem.-Eur. J.* **2011**, *17*, 14326. [[CrossRef](#)] [[PubMed](#)]
169. Barbosa, J.C.; Goncalves, R.; Costa, C.M.; Bermudez, V.D.; Marijuan, A.F.; Zhang, Q.; Mendez, S.L. Metal-organic framework, and zeolite materials as active fillers for lithium-ion battery solid polymer electrolytes. *Mater. Adv.* **2021**, *2*, 3790–3805. [[CrossRef](#)]
170. Mazzapioda, L.; Sgambetterra, M.; Tsurumaki, A.; Navarra, M.A. Different approaches to obtain functionalized alumina as additive in polymer electrolyte membranes, Different approaches to obtain functionalized alumina as additive in polymer electrolyte membranes. *J. Solid State Electrochem.* **2022**, *26*, 17–27. [[CrossRef](#)]
171. Zhou, H.; Wang, Y.; Li, H.; He, P. The Development of a new type of rechargeable batteries based on Hybrid electrolytes. *ChemSusChem* **2010**, *3*, 1009–1019. [[CrossRef](#)]
172. Manthiram, A.; Yu, X.; Wang, S. Lithium battery chemistries enabled by solid-state electrolytes. *Nat. Rev. Mater.* **2017**, *2*, 16103. [[CrossRef](#)]
173. Han, L.; Lehmann, M.L.; Zhu, J.; Liu, T.; Zhou, Z.; Tang, X.; Heish, C.-T.; Sokolov, A.P.; Cao, P.; Chen, X.C.; et al. Recent developments, and challenges in hybrid solid electrolytes for Lithium-ion batteries. *Front. Energy Res.* **2020**, *8*, 202. [[CrossRef](#)]
174. Kwon, T.; Choi, I.; Park, M.J. Highly Conductive Solid-state hybrid electrolytes operating at subzero temperature. *ACS Appl. Mater. Interfaces* **2017**, *9*, 24250–24258. [[CrossRef](#)]
175. Janek, J.; Zeier, W.G. A solid future battery development. *Nat. Energy* **2016**, *1*, 16141. [[CrossRef](#)]
176. Liu, H.; Sun, Q.; Zhang, H.; Cheng, J.; Li, Y.; Zeng, Z.; Zhang, S.; Xu, X.; Ji, F.; Li, D.; et al. The application road of silicon-based anode in lithium-ion batteries: From liquid electrolyte to solid-state electrolyte. *Energy Storage Mater.* **2023**, *55*, 244–263. [[CrossRef](#)]
177. Murugan, R.; Thangadurai, V.; Weppner, W. Fast Lithium Ion Conduction in Garnet-Type  $\text{Li}_7\text{La}_3\text{Zr}_2\text{O}_{12}$ . *Angew. Chem. Int. Ed.* **2007**, *46*, 7778–7781. [[CrossRef](#)]
178. Kim, K.H.; Iriyama, Y.; Yamamoto, K.; Kumazaki, S.; Asaka, T.; Tanabe, K.; Fisher, C.A.J.; Hirayama, T.; Murugan, R.; Ogumi, Z. Characterization of the interface between  $\text{LiCoO}_2$  and  $\text{Li}_7\text{La}_3\text{Zr}_2\text{O}_{12}$  in an all-solid-state rechargeable lithium battery. *J. Power Sources* **2011**, *196*, 764–767. [[CrossRef](#)]
179. Ihrig, M.; Kuo, L.-Y.; Lobe, S.; Laptev, A.M.; Lin, C.-A.; Tu, C.-H.; Ye, R.; Kaghazchi, P.; Cressa, L.; Eswara, S.; et al. Thermal Recovery of the Electrochemically Degraded  $\text{LiCoO}_2/\text{Li}_7\text{La}_3\text{Zr}_2\text{O}_{12}:\text{Al/Ta}$  Interface in an All-Solid-State Lithium Battery. *ACS Appl. Mater. Interfaces* **2023**, *15*, 4101–4112. [[CrossRef](#)]
180. Teng, Y.; Liu, H.; Wang, Q.; He, Y.; Hua, Y.; Li, C.; Bai, J. In-doped  $\text{Li}_7\text{La}_3\text{Zr}_2\text{O}_{12}$  nanofibers enhances electrochemical properties and conductivity of PEO-based composite electrolyte in all-solid-state lithium battery. *J. Energy Storage* **2024**, *76*, 109784. [[CrossRef](#)]

181. Morimoto, H.; Yamashita, H.; Tatsumisago, M.; Minami, T. Mechanochemical Synthesis of New Amorphous Materials of  $60\text{Li}_2\text{S}\text{-}40\text{SiS}_2$  with High Lithium Ion Conductivity. *J. Am. Ceram. Soc.* **1999**, *82*, 1352–1354. [[CrossRef](#)]
182. Wheaton, J.; Martin, S.W. Impact of impurities on the thermal properties of a  $\text{Li}_2\text{S}\text{-}\text{SiS}_2\text{-}\text{LiPO}_3$  glass. *Appl. Glass Sci.* **2024**, *15*, 317–328. [[CrossRef](#)]
183. Olson, M.; Kmiec, S.; Riley, N.; Oldham, N.; Krupp, K.; Manthiram, A.; Martin, S.W. Structure and Properties of  $\text{Na}_2\text{S}\text{-}\text{SiS}_2\text{-}\text{P}_2\text{S}_5\text{-}\text{NaPO}_3$  Glassy Solid Electrolytes. *Inorg. Chem.* **2024**, *63*, 9129–9144. [[CrossRef](#)]
184. Zhang, X.; Wang, S.; Xue, C.; Xin, C.; Lin, Y.; Shen, Y.; Li, L.; Nan, C.-W. Self-Suppression of Lithium Dendrite in All-Solid-State Lithium Metal Batteries with Poly(vinylidene difluoride)-Based Solid Electrolytes. *Adv. Mater.* **2019**, *31*, 186082. [[CrossRef](#)]
185. Tang, Y.; Xiong, Y.; Wu, L.; Xiong, X.; Me, T.; Wang, X. A Solid-State Lithium Battery with PVDF–HFP-Modified Fireproof Ionogel Polymer Electrolyte. *ACS Appl. Energy Mater.* **2023**, *6*, 4016–4026. [[CrossRef](#)]
186. Tran, H.K.; Truong, B.T.; Zhang, B.-R.; Jose, R.; Chang, J.-K.; Yang, C.-C. Sandwich-Structured Composite Polymer Electrolyte Based on PVDF-HFP/PPC/Al-Doped LLZO for High-Voltage Solid-State Lithium Batteries. *ACS Appl. Energy Mater.* **2023**, *6*, 1475–1487. [[CrossRef](#)]
187. Liu, Y.; Xu, X.; Jiao, X.; Kapitanova, O.O.; Song, Z.; Xiong, S. Role of Interfacial Defects on Electro-Chemo-Mechanical Failure of Solid-State Electrolyte. *Adv. Mater.* **2023**, *35*, 2301152. [[CrossRef](#)] [[PubMed](#)]
188. Xiong, S.; Xu, X.; Jiao, X.; Wang, Y.; Kapitanova, O.O.; Song, Z.; Liu, Y. Mechanical Failure of Solid-State Electrolyte Rooted in Synergy of Interfacial and Internal Defects. *Adv. Energy Mater.* **2023**, *13*, 2203614. [[CrossRef](#)]
189. Akhtar, S.; Lee, W.; Kim, M.; Park, M.S.; Yoon, W.-S. Conduction Mechanism of charge carriers in electrodes and design factors for the improvement of charge conduction in Li-Ion batteries. *J. Electrochem. Sci. Technol.* **2021**, *12*, 1–20. [[CrossRef](#)]
190. Zhang, Y.; Tao, L.; Xie, C.; Wang, D.; Zou, Y.; Chen, R.; Wang, Y.; Jia, C.; Wang, S. Defect Engineering on Electrode Materials for rechargeable batteries. *Adv. Mater.* **2020**, *32*, 1905923. [[CrossRef](#)]
191. Guo, W.; Meng, Y.; Hu, Y.; Wu, X.; Ju, Z.; Zhuang, Q. Surface, and Interface modification of electrode materials for lithium-ion batteries with organic liquid electrolytes. *Front. Energy Res.* **2020**, *8*, 170. [[CrossRef](#)]
192. Nasir, U.; Muralidharan, N.; Essehli, R.; Amin, R.; Belharouak, I. Valuation of Surface Coatings in High-Energy Density Lithium-Ion battery cathode Materials. *Energy Storage Mater.* **2021**, *38*, 309–328.
193. Vu, A.; Qian, Y.; Stein, A. Porous Electrode Materials for Lithium-Ion Batteries How to Prepare Them and What makes them Special. *Adv. Energy Mater.* **2012**, *2*, 1056–1085. [[CrossRef](#)]
194. Du, H.-L.; Jeong, M.-G.; Lee, Y.-S.; Choi, W.; Lee, J.K.; Oh, I.-H.; Jung, H.-G. Coating lithium titanate with nitrogen-doped carbon by simple refluxing for high-power lithium-ion batteries. *ACS Appl. Mater. Interfaces* **2015**, *7*, 10250–10257. [[CrossRef](#)]
195. Xu, K.; Wang, C. Batteries: Widening voltages windows. *Nat. Energy* **2016**, *1*, 16161. [[CrossRef](#)]
196. Gao, J.; Shi, S.-Q.; Li, H. Brief overview of electrochemical potential in lithium-ion batteries. *Chin. Phys. B* **2016**, *25*, 018210. [[CrossRef](#)]
197. Ven, A.V.D.; Bhattacharya, J.; Belak, A.A. Understanding Li Diffusion in Li-ion Intercalation compounds. *Acc. Chem. Res.* **2013**, *46*, 1216–1225.
198. Dong, C.; Xu, F.; Chen, L.; Chen, Z.; Cao, Y. Design Strategies for High-Voltage Aqueous batteries. *Small Struct.* **2021**, *2*, 2100001. [[CrossRef](#)]
199. Melot, B.C.; Tarascon, J.-M. Design and Preparation of Materials for Advanced Electrochemical Storage. *Acc. Chem. Res.* **2013**, *46*, 1226–1238. [[CrossRef](#)] [[PubMed](#)]
200. Masquelier, C.; Croguennec, L. Polyanionic (Phosphates, Silicates, Sulfates) Frameworks as Electrode materials for rechargeable Li (or Na) Batteries. *Chem. Rev.* **2013**, *113*, 6552–6591. [[CrossRef](#)]
201. Liu, C.; Neale, Z.G.; Cao, G. Understanding electrochemical potentials of cathode materials in rechargeable batteries. *Mat. Today* **2016**, *19*, 109–123. [[CrossRef](#)]
202. Yazami, R. *Nanomaterials for Lithium-Ion Batteries: Fundamentals and Applications*; CRC Press, Taylor & Francis Group: Boca Raton, FL, USA, 2013.
203. Park, J.-K. *Principles, and Applications of Lithium Secondary Batteries*; Wiley-VCH: Weinheim, Germany, 2012.
204. Hahn, B.P.; Long, J.W.; Rolison, D.R. Something from Nothing: Enhancing Electrochemical Charge Storage with Cation Vacancies. *Acc. Chem. Res.* **2013**, *46*, 1181–1191. [[CrossRef](#)]
205. Tang, Y.; Zhang, Y.; Li, W.; Ma, B.; Chen, X. Rational material design for ultrafast rechargeable lithium-ion batteries. *Chem. Soc. Rev.* **2015**, *44*, 5926–5940. [[CrossRef](#)]
206. Kim, I.G.; Ghani, F.; Lee, K.-Y.; Park, S.; Kwak, S.; Kim, H.-S.; Nah, I.W.; Lim, J.C. Electrochemical performance of  $\text{Mn}_2\text{O}_3$  nanorods by N-doped reduced graphene oxide using ultrasonic spray pyrolysis for lithium storage. *Intl. J. Energy Res.* **2020**, *44*, 11171–11184. [[CrossRef](#)]
207. Cao, K.; Jin, T.; Yang, L.; Jiao, L. Recent progress in Conversion reaction metal oxide anodes for Li-ion batteries. *Mater. Chem. Front.* **2017**, *1*, 2213–2242. [[CrossRef](#)]
208. Ghani, F.; Nah, I.W.; Kim, H.-S.; Lim, J.C.; Marium, A.; Ijaz, M.F.; Rana, A.H.S. Facile one-step hydrothermal synthesis of rGO@ $\text{Ni}_3\text{V}_2\text{O}_8$  interconnected hollow microspheres composite for lithium-ion batteries. *Nanomaterials* **2020**, *10*, 2389. [[CrossRef](#)] [[PubMed](#)]
209. He, L.-P.; Sun, S.-Y.; Song, X.-F.; Yu, J.-G. Recovery of cathode materials and Al from spent lithium-ion batteries by ultrasonic cleaning. *Waste Manag.* **2015**, *46*, 523–528. [[CrossRef](#)] [[PubMed](#)]

210. Liu, H.; Cheng, X.; Chong, Y.; Yuan, H.; Huang, J.-Q.; Zhang, Q. Advanced electrode processing of lithium-ion batteries: A review of powder technology in battery fabrication. *Particuology* **2021**, *57*, 56–71. [[CrossRef](#)]
211. Goncalves, R.; Mendez, S.L.; Costa, C.M. Electrode fabrication process and its influence in lithium-ion battery performance: State of the art and future trends. *Electrochim. Comm.* **2022**, *135*, 107210. [[CrossRef](#)]
212. Liu, Y.; Zhang, R.; Wang, J.; Wang, Y. Current and future lithium-ion battery manufacturing. *iScience* **2021**, *24*, 102332. [[CrossRef](#)]
213. Gonçalves, R.; Dias, P.; Hilliou, L.; Costa, P.; Silva, M.M.; Costa, C.M.; Galvan, S.C.; Mendez, S.L. Optimized printed cathode electrodes for high performance batteries. *Energy Technol.* **2021**, *9*, 2000805. [[CrossRef](#)]
214. Lalau, C.C.; Low, C.T.J. Electrophoretic deposition for lithium-ion battery electrode manufacture. *Batter. Supercaps* **2019**, *2*, 551–559. [[CrossRef](#)]
215. Goren, A.; Juarez, D.C.; Martins, P.; Ferdov, S.; Silva, M.M.; Tirado, J.L.; Costa, C.M.; Mendez, S.L. Influence of solvent evaporation rate in the preparation of carbon-coated lithium iron phosphate cathode films on battery performance. *Energy Technol.* **2016**, *4*, 573–582. [[CrossRef](#)]
216. Meyer, C.; Bockholt, H.; Haselrieder, W.; Kwade, A. Characterization of the calendaring process for compaction of electrodes for lithium-ion batteries. *J. Mater. Process. Technol.* **2017**, *249*, 172–178. [[CrossRef](#)]
217. Jeon, D.H. Wettability in electrodes and its impact on the performance of lithium-ion batteries. *Energy Storage Mater.* **2019**, *18*, 139–147. [[CrossRef](#)]
218. Robles, D.J.; Vyas, A.A.; Fear, C.; Jeevarajan, J.A.; Mukherjee, P.P. Overcharge and Aging Analytics of Li-Ion Cells. *J. Electrochem. Soc.* **2020**, *167*, 090547. [[CrossRef](#)]
219. Qian, J.; Liu, L.; Yang, J.; Li, S.; Wang, X.; Zhuang, H.L.; Lu, Y. Electrochemical surface passivation of LiCoO<sub>2</sub> particles at ultrahigh voltage and its applications in lithium-based batteries. *Nat. Commun.* **2018**, *9*, 4918. [[CrossRef](#)]
220. Yu, F.; Wang, Y.; Guo, C.; Liu, H.; Bao, W.; Li, J.; Zhang, P.; Wang, F. Spinal LiMn<sub>2</sub>O<sub>4</sub> cathode materials in wide voltage window: Single-Crystalline versus Polycrystalline. *Crystals* **2022**, *12*, 317. [[CrossRef](#)]
221. Hu, L.-H.; Wu, F.-Y.; Lin, C.; Khlobystov, A.N.; Li, L.-J. Graphene-modified LiFePO<sub>4</sub> cathode for lithium-ion battery beyond theoretical capacity. *Nat. Commun.* **2013**, *4*, 1687. [[CrossRef](#)]
222. Song, H.; Li, J.; Luo, M.; Zhao, Q.; Liu, F. Ultra-Thin mesoporous LiV<sub>3</sub>O<sub>8</sub> Nanosheet with exceptionally large specific area for fast and reversible Li storage in Lithium-ion battery cathode. *J. Electrochem. Soc.* **2021**, *168*, 050515. [[CrossRef](#)]
223. Wu, X.; Song, K.; Zhang, X.; Hu, N.; Li, L.; Li, W.; Zhang, L.; Zhang, H. Safety Issues in Lithium-Ion Batteries: Materials and cell Design. *Front. Energy Res.* **2019**, *7*, 65. [[CrossRef](#)]
224. Kim, C.-S.; Jeong, K.M.; Kim, K.; Yi, C.-W. Effects of Capacity ratios between anode and cathode on electrochemical properties for lithium polymer batteries. *Electrochim. Acta* **2015**, *155*, 431–436. [[CrossRef](#)]
225. Fanfeng, L.; Cheng, C.; Zhiyuan, Z.; Weikang, Z.; Zhengzhong, L.Y.U. The influence of N/P ratio on the performance of lithium iron phosphate batteries. *Energy Storage Sci. Technol.* **2021**, *10*, 1325–1329.
226. Angelopoulou, P.; Avgouropoulos, G. Effect of electrode loading on the electrochemical performance of LiAl<sub>0.1</sub>Mn<sub>1.9</sub>O<sub>4</sub> Cathode for lithium-ion batteries. *Mater. Res. Bull.* **2019**, *119*, 110562. [[CrossRef](#)]

**Disclaimer/Publisher's Note:** The statements, opinions and data contained in all publications are solely those of the individual author(s) and contributor(s) and not of MDPI and/or the editor(s). MDPI and/or the editor(s) disclaim responsibility for any injury to people or property resulting from any ideas, methods, instructions or products referred to in the content.